214-0112-01-01_00

RF Note 111 February 1992
F. Pigeaud

I. K500 3rd Harmonic Flat-Topping Study.

This paper documents the RF analysis of a third harmonic accelerating structure for possible installation in the NSCL K500 cyclotron. The preliminary study is being performed on the K500 in order to assess its feasibility and infer what success this technique may have with the K1200 cyclotron. The technique of adding a third harmonic acceleration component is termed 'flat-topping' because the aim is to flatten the energy distribution over RF phase angle.

When accelerating at a single frequency, the distribution of energy versus initial phase for each turn is sinusoidal near the peak energy value. Since energy is a function of radius, a similar distribution can be drawn with radius as the ordinate, giving a series of curves corresponding to each turn. Beam extraction occurs over a span of radius which implies multiple turns are extracted for a discrete segment of phase.

If, however, the particle energy versus phase curves are 'flat', the energy will vary less with initial phase, and so the same window in radius will extract the peak energy particles for a greater fraction of the RF period. In the ideal case, the entire beam could be extracted at a narrow radius (single turn), with all particles having the same energy, regardless of initial phase. In order to approach this ideal flat (square wave) distribution, the first odd harmonic of the fundamental can be added as in a Fourier series. A fundamental frequency of 17.76MHz was chosen for this analysis, which corresponds to an energy of approximately 30 Mev/u and a third harmonic component of 53.28MHz.

The third harmonic accelerating gap sits between the dee shell and a plate which runs along the inside of this shell. From an RF standpoint the dee shell becomes the outer conductor of the flat-topping structure, while the plate acts as the inner conductor. The flat-topping structure is referred to as the 'sub-dee' in this paper. A tuning stem connects to the middle of the plate and extends up inside the dee shell where it is shorted. The sub-dee equivalent model was analyzed with the NSCL software RFA and RESON to determine parameters such as power loss, resonant frequency, etc. The main design criteria and results are briefly discussed here, with a more complete discussion found in the following sections.

Dee Coupling.

Since the upper and lower sub-dees cannot be physically connected together, the first design consideration was whether to drive each dee separately, or to couple them together and drive from one side. Simulations indicated that the dee-to-dee capacitance was great enough to provide good coupling without a large voltage drop across the median plane. Additionally, driving

from one side simplifies mechanical constraints.

Power Feed and Tuning.

The power and feedback signals for the resonator would have to be brought down the inside of the main dee inner conductor. This imposed many restrictions on the design of the coupling structure and tuning arrangement. Analysis of this problem indicated that even mode coupling is a necessity, since it allows power to be delivered down the upper stem only. It is important to couple into the upper stem because, from the this side, one can make initial tuning adjustments on the entire two dee structure while the cyclotron cap is up. This is not feasible from the lower stem side. Another important restriction imposed on the design is that the sub-dee short must not extend beyond the dee shell so there is sufficient space for the mechanical assemblies.

Dee Support.

The inner conductor of the sub-dee stem probably cannot support the plate because it will have too small a crossection. The size of this inner conductor is set by tuning requirements, and power loss considerations, leaving little room for adjustment. Support for the plate will have to be provided by insulated stand-offs, preferably of greyed alumina.

Power Requirements.

Simulations indicated that the losses are approximately 800W per dee with 20kV peak at the center of each sub-dee. Using conservative estimates this would amount to an RF amplifier capable of supplying 2-3KW for the entire system. Complete tube driven transmitters at this power level are available for $5-6000, though they have a limited bandwidth (~1MHz). This transmitter, however, could be retro-fitted at the lab to allow for greater tuning range.

II. Circuit Model.

The first step in the analysis was to break the sub-dee into discrete transmission line sections for analysis in RESON, a PC-based circuit simulator written at the NSCL. A top view of the K500 dee shell is shown in figure A.1, with crossection names and locations indicated on the drawing. The relationship between these crossection locations and the equivalent transmission lines is shown in figures A.2, A.3. The dimensions of each crossection were determined from the available dee shell drawings, assuming a flat plate for the inner conductor. The plate was rounded at the gap edge to a 1 cm diameter and the gap itself is 1 cm wide along the entire edge of the conductor. These crossections are shown in Appendix D.

The equivalent transmission line characteristics of each of these sections was determined using a PC version of POISSON which was improved at the NSCL to provide additional information such as charge distribution. Using field plots and POISSON data the characteristic impedance of each section was determined, as well as the equivalent conductor boundary lengths. The equivalent boundary length is the actual boundary divided by a constant termed the 'R factor'. This factor adjusts the inner and outer transmission line crossection boundary lengths to account for conductor losses due to inhomogeneous current distributions. A list of the transmission line parameters is provided in table A.1. The POISSON input files for each of these sections is included in Appendix E.

III. Single Dee Analysis.

A single dee structure was analyzed to determine the losses and required stem length. The RESON input file (FLT4.dat) is included in Appendix B. The significant results are; approximately 800W are dissipated by conductor losses in each sub-dee with 20kV peak at the sub-dee midpoint, and the stem short for this case is positioned about 15 cm above the K500 median plane (see figure C.3). This stem position is for a stem center conductor which consists of three 1/4" O.D. tubes located side-by-side: a supply and return water line plus a coaxial conductor which feeds the coupling loop. If the center conductor's effective inner radius is increased beyond these dimensions several undesirable effects will result. As the inductance of this line is reduced the stem length will increase, placing it closer to, or above the dee shell top. The access to the coupling loop and water lines will then be too severely restricted. Additionally, if the stem transmission line protrudes above the dee shell it will have a greatly reduced crossection causing increased power loss at the shorted end.

It is therefore important to maintain the equivalent lumped reactances near the present values in order to mechanically fit the structure into the K500 system. This point will be important later if trimming is done to the sub-dee structure in order to balance the voltage across its length. For example, if the accelerating

gap length is changed the dee capacitance will change, resulting in a new stem position which must remain within the dee shell.

For the nominal dee voltage (20kV peak), the shorted section of the sub-dee stem (TL11 in figure A.3) dissipates about 220W, while the subsequent section of line (TL10) dissipates 280W. Most of this dissipation occurs on the center conductor due to its smaller surface area. A rough estimate is that half the total power is dissipated on the inner conductor along its length from the short to the inner conductor (about 12 cm long), and the rest is dissipated on the dee shell and the sub-dee plate. The total power dissipated by the sub-dee would correspond to a three or four Centigrade temperature rise at 1 GPM. It is assumed that a tee junction can be made off the main dee water line to cool this circuit.

IV. Two Dee Analysis.

To test the feasibility of even mode coupling between the dees, the dee-to-dee capacitance was estimated using the ideal parallel plate relation. Given a surface area of approximately 2236 square cm and a gap between dees of 2.8 cm, the capacitance works out to 70 pF. This capacitance was distributed across the length of the dee as shown in figure B.1. The two dee RESON input file (FLT5.DAT) is listed in Appendix B. The two coupled modes have the following characteristics:

Even mode:	f0 = 53.28 MHz
	Q = 3300
Odd mode:	f0 = 29.21 MHz
	Q = 2660

The first issue to addressed in this analysis was how much the voltage differed between the upper and lower dees. This is a function of the dee-to-dee capacitance and how it is distributed in the model. As shown in figure B.1 the capacitance was defined at nine discreet points, and sums to 70pF. For this large a capacitance the voltage difference was less than one volt along the entire dee. An important characteristic of the dees determined at this point was the voltage distribution along a single dee. As shown in figure B.2 the voltage varies by as much as 140% over the length of the dee.

The shift in resonant frequency due to stem length changes was also determined in this study. The dee structure and stems will be built according to simulation results and assembled, without tuning allowances. Since the test does not need a very specific frequency its assumed we will perform the study with the mode which resonates on turn-on. From past experience the actual frequency should not differ from the simulation results by more than a few percent if the mechanical dimensions accurately reflect the design. A change in the lower dee short position was analyzed to give a feel for

relative mechanical shifts and their effect on the resonant frequency. Figure B.3 shows the variation in the resonant frequency of the cavity when the upper stem length is held constant (i.e. the length of t-line 11 is 4.7 cm), and the lower stem (t-line 11L) length is shifted from its nominal setting. The subsequent graph, figure B.4, illustrates how the voltage drop across the median plane will vary when resonance is shifted by moving the lower stem only. From these results we can see that mechanical error in the assembly will not cause a significant shift in the predicted fundamental mode or voltage drop across the dees.

V. Coupling and Monitoring.

Coupling will be achieved through a loop in the upper stem assembly, while monitoring will be done through a pick-up loop in the lower stem. The reason for using the upper stem for coupling was addressed briefly in the introduction: with the cap up, the entire dee structure will remain intact, so adjustments and measurements can easily be made. The only planned adjustment for the system is a variation in the position or angle of the coupling loop so as to match the cavity to the feed line. Once this is done the loop can be locked in position permanently. Eliminating tuning adjustments eases the mechanical design since there will be no moving parts or vacuum feedthroughs to bother with in this very confined space.

A detailed description of the mechanical aspects of the coupling loop was not completed in this report. That element of the design will be addressed at a later phase in conjunction with mechanical design personnel. Figure C.2 shows the current configuration of the K500 dee near the stem interface, while figure C.3 depicts two crossectional views of the proposed coupling components and inner conductor. Calculations of the approximate loop area and position were completed and are included in Appendix C.

Appendix A. POISSON/RFA Analysis.

This appendix contains information about the analysis of the dee crossections and equivalent transmission line parameters. Figure A.1 shows a top view of the K500 dee shell, with the applicable crossections indicated. Straight line connections were drawn between the approximate center of each crossection in order to estimate the length of each transmission line. As shown in figure A.2, each equivalent transmission line is centered on the crossection which defines its parameters (Z0, etc.) Figure A.3 illustrates the arrangement of a single dee transmission line model with the stem sections included. For views of the dee which define the stem sections, refer to the appropriate drawings under Appendix C.

Drawings of each of the dee crossections are included at the end of this report in Appendix D. These views are output from the PC based software, POISSON-386. Enclosed in Appendix E are the input data files used for the POISSON analysis of each section.

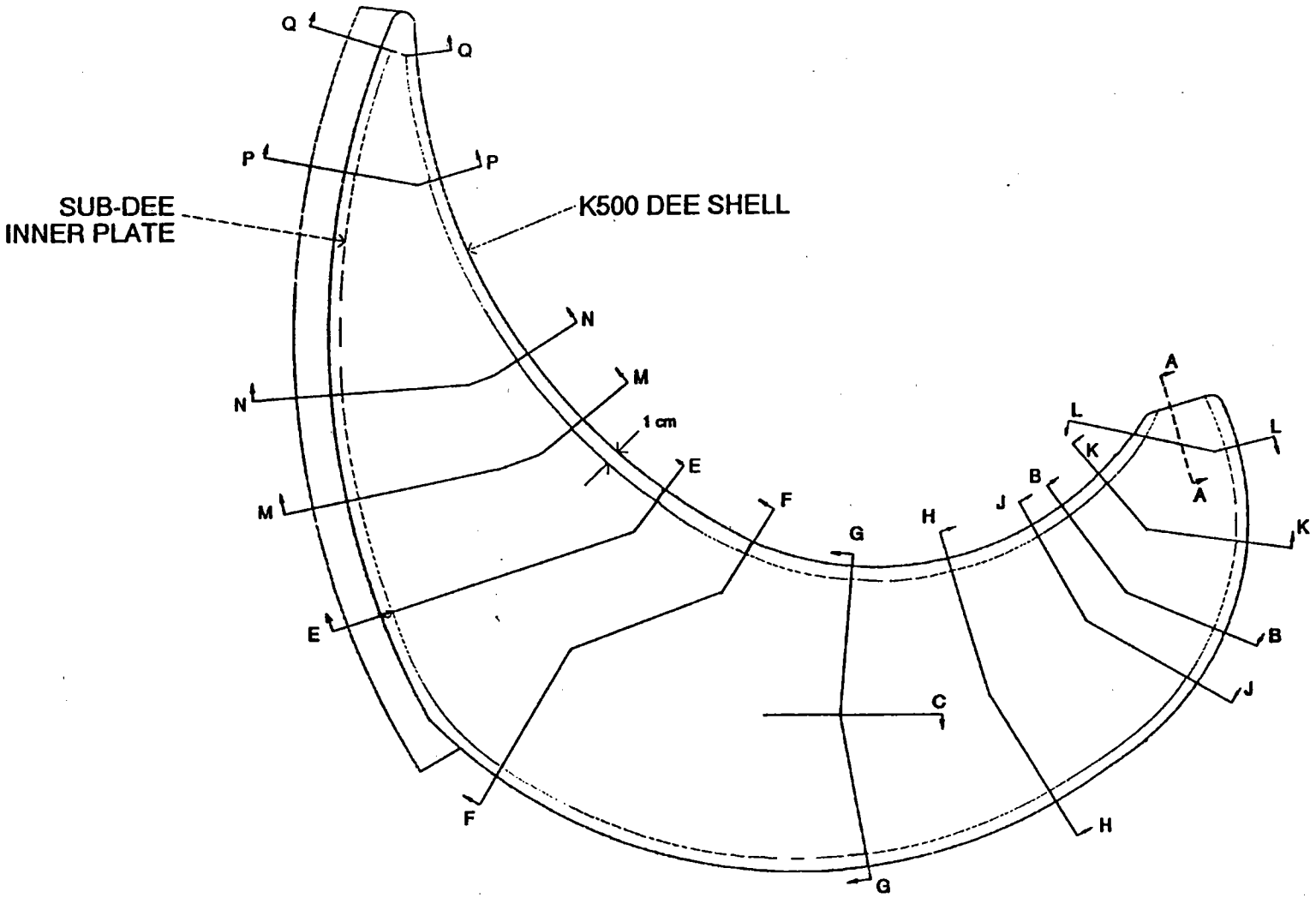

Figure A.1 K500 Dee Cross-sections

Figure A.2 SUB–DIVISION OF DEE

lengths in cm.

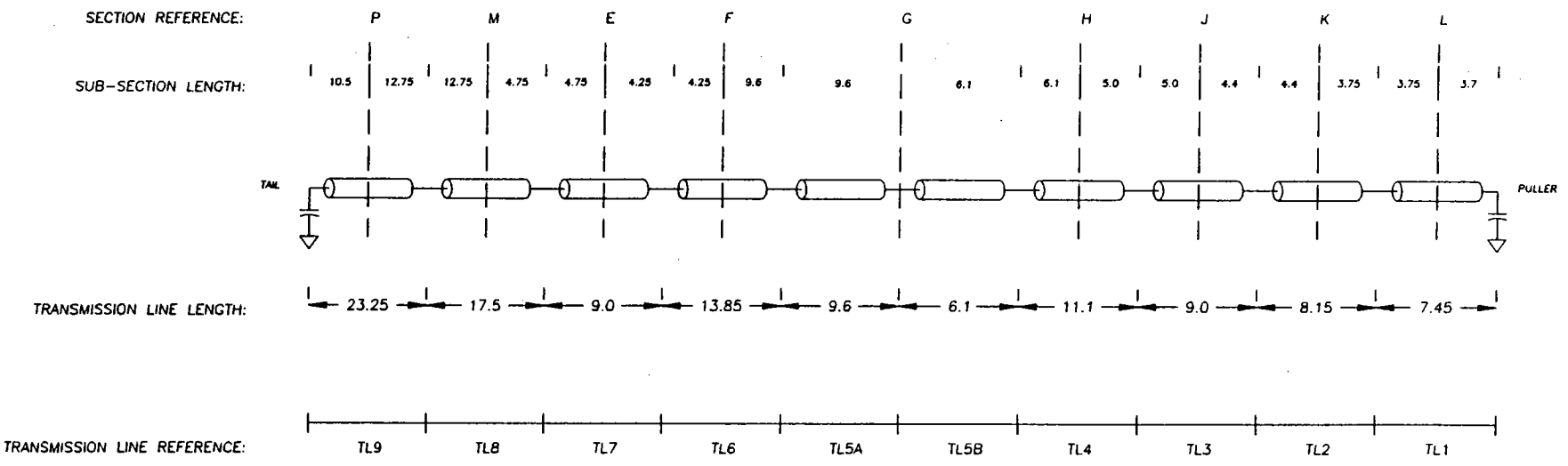

Figure A.3 SINGLE SUB-DEE TRANSMISSION LINE ARRANGEMENT .
Showing lengths [cm] and associated crossection references.

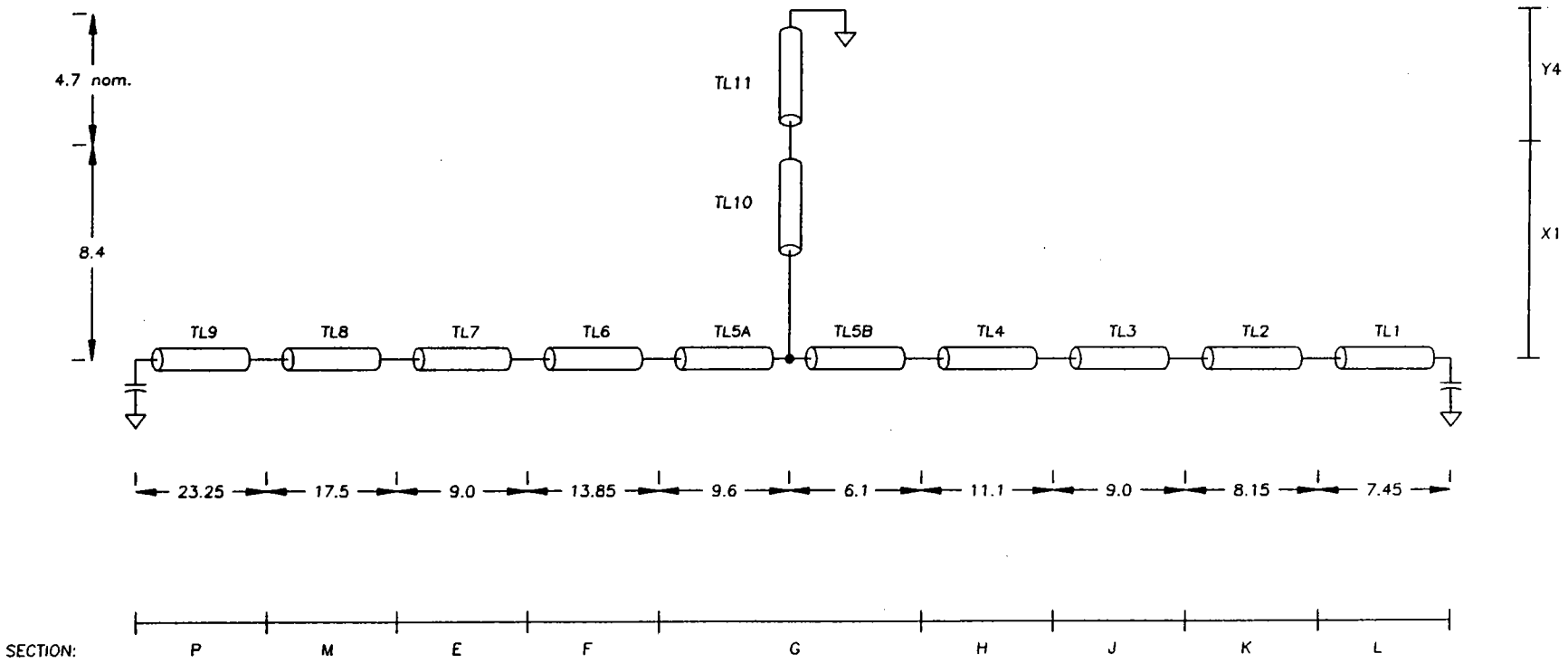

TABLE A.1 CROSSECTION PARAMETERS.
As determined by E-field plots and RFA results.

crossection label	inner conductor				outer conductor				average	Zo	T-line
	charge [pC]	boundary length [cm]	R factor	length/Rfactor [cm]	charge [pC]	boundary length [cm]	R factor	length/Rfactor [cm]	charge [pC]	[Ohms]	reference
E1	50.3	44.2	4.3	10.3	62.4	43.5	1.9	22.9	56.4	59.2	TL7
F1	52.2	54.2	4.6	11.8	64.2	46.8	1.8	26.0	58.2	57.3	TL6
G1	53.8	45.8	3.8	12.1	58.4	41.8	1.7	24.6	56.1	59.4	TL5
H1	46	38.4	4	9.6	50	38.4	1.6	24.0	48.0	69.4	TL4
J1	47.8	33.4	4	8.4	45.8	37	1.9	19.5	46.8	71.2	TL3
K1	43.4	23.4	3.5	6.7	39.2	31.4	2.2	14.3	41.3	80.7	TL2
L1	46.4	9.5	1.9	5.0	43.6	28.9	3.1	9.3	45.0	74.1	TL1
M1	49.3	33.2	2.3	14.4	49.6	36.4	1.6	22.7	49.5	67.4	TL8
P1	40.3	10.9	1.9	5.7	35	20.8	1.9	10.9	37.7	88.5	TL9
X1 (1)	6.2	5.9	1	5.9	9.8	71.9	1	71.9	8.0	416.7	TL10
Y4 (2)	26.6	4.5	1	4.5	26.6	33.0	1	33.0	26.6	125.3	TL11

Notes:

Data on sections E1-P1 is for single sub-dee structure (upper or lower).

(1) Equivalent length calculations shown on following pages.

(2) R factor calculation assumes essentially concentric conductors.

Notes on Crossection X1 Equivalent Length.

Since there are two separate return paths for this conductor system, the total equivalent boundary length is a weighted sum of these two lengths. The distribution of current on the surfaces can be inferred from the charge distribution information provided by the RFA output. For this calculation the return current is normalized to 1 amp.

$$conductor\ 1\ current:\ I_1 = \frac{Q_1}{Q_1+Q_2} = 0.46$$

$$conductor\ 2\ current\ I_2:\ = 0.54$$

The power dissipated on each conductor must sum to the total power dissipated by one amp on a conductor of equivalent length Leqo.

$$I_1^2\left(\frac{R_s R_{f1}}{L_1}\right)+I_2^2\left(\frac{R_s R_{f2}}{L_2}\right) = (1)^2\left(\frac{R_s R_{fo}}{L_o}\right)$$

where
- Rs = surface resistivity
- Rf1, Rf2 = R-factor of surface 1, 2
- L1, L2 = actual boundary length of cond.1, 2
- Rfo = total outer conductor R-factor
- Lo = L1 + L2

The total equivalent outer boundary length is then given by

$$L_{eqo} = \frac{L_o}{R_{fo}} = \frac{1}{I_1^2\left(\frac{R_{f1}}{L_1}\right)+I_2^2\left(\frac{R_{f2}}{L_2}\right)} = 71.9\,cm$$

Appendix B. RESON Simulation.

This appendix contains information about the RESON simulation results. Figure B.1 shows the two dee model with the element names as used in the input files. The next pages include the input files for the two major simulations which were completed. The first file, FLT4.DAT, is for the single dee structure which was used for preliminary analysis of resonant frequency and losses. The second file, FLT5.DAT, is the complete two dee model which was used primarily to look at even mode coupling characteristics, and input coupler properties.

Several results from the RESON analyses are also included in this section. The graph in figure B.2 displays the variation in dee voltage across the length of the dee. This large variation occurs because the dee length is an appreciable fraction of the wavelength. From a beam dynamics view, a more optimum distribution of energy gain versus radius might be achieved by varying the dee voltage along its length. Such a variation with length could be achieved by varying the characteristic impedance of the dee.

The other figures enclosed (B.3 and B.4) show results from the frequency shift versus stem length analysis.

Figure B.1 Transmission Line Model of Coupled Dees.

RESON input file: FLT5.DAT

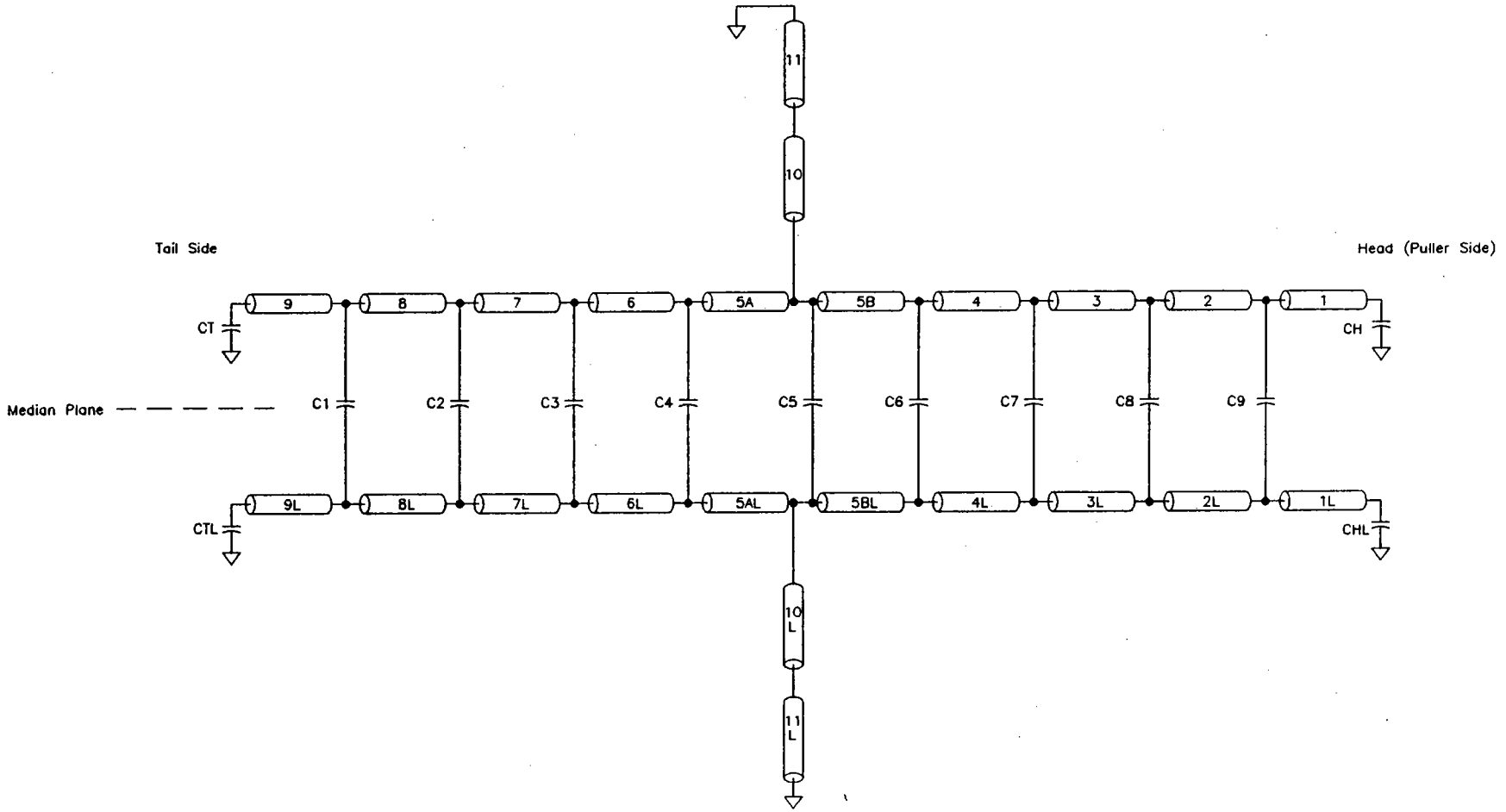

FIGURE B.2 DEE VOLTAGE vs. POSITION

K500 3RD HARMONIC ANALYSIS

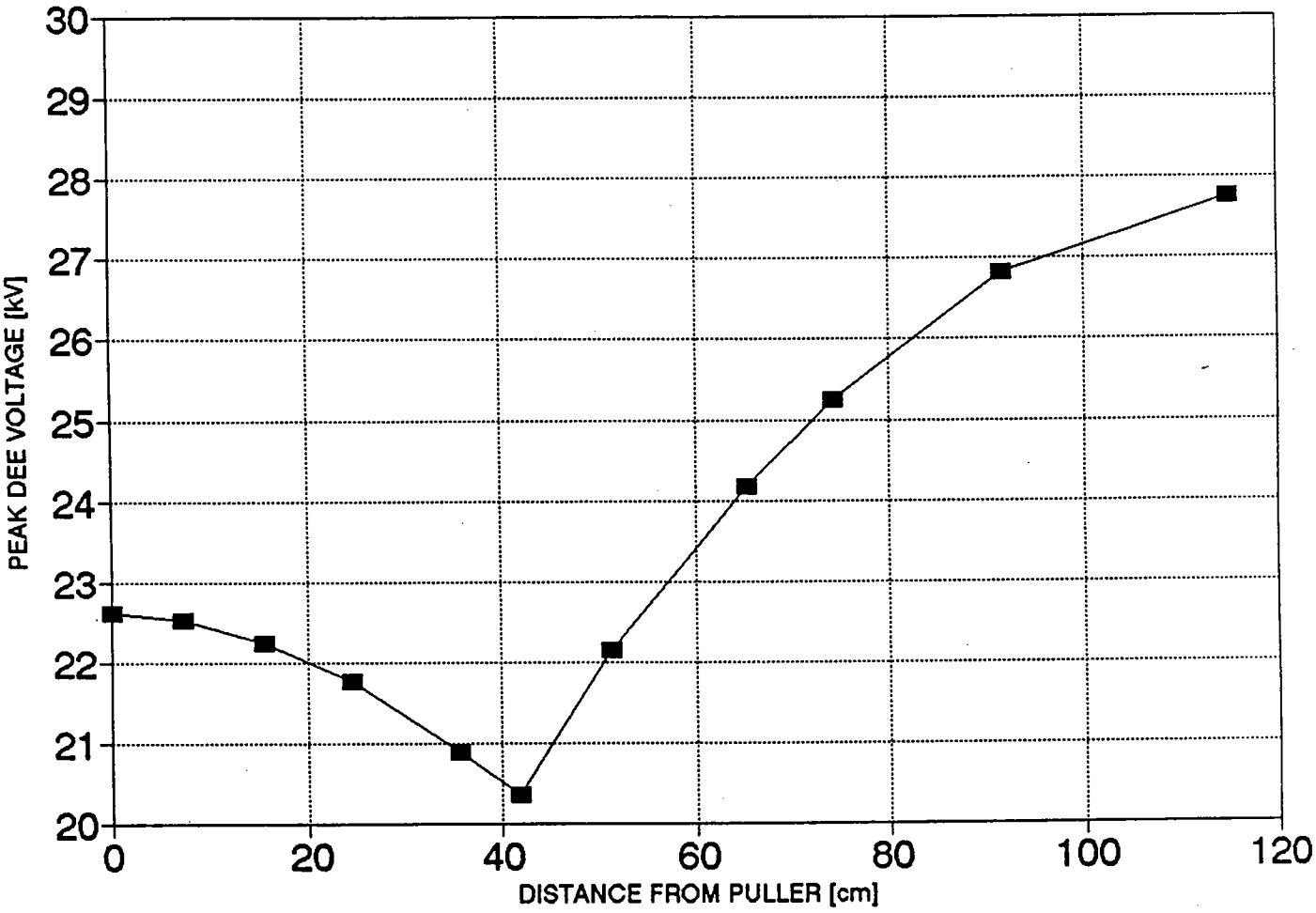

FIGURE B.3 STEM LENGTH vs. FREQUENCY

Upper stem length contant (4.706 cm)

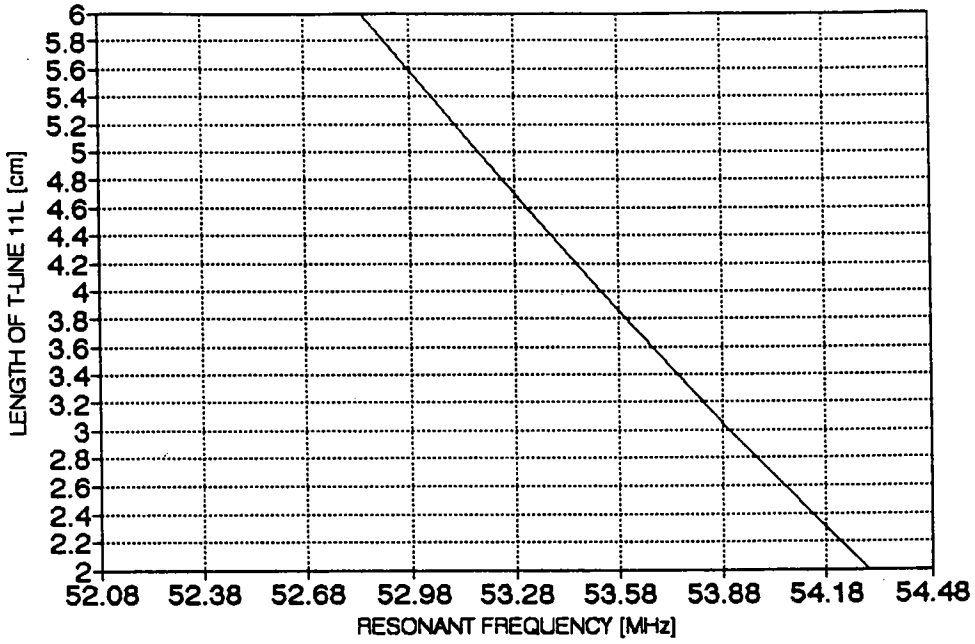

FIGURE B.4 VOLTAGE DROP vs. FREQUENCY

Upper stem length contant (4.706 cm)

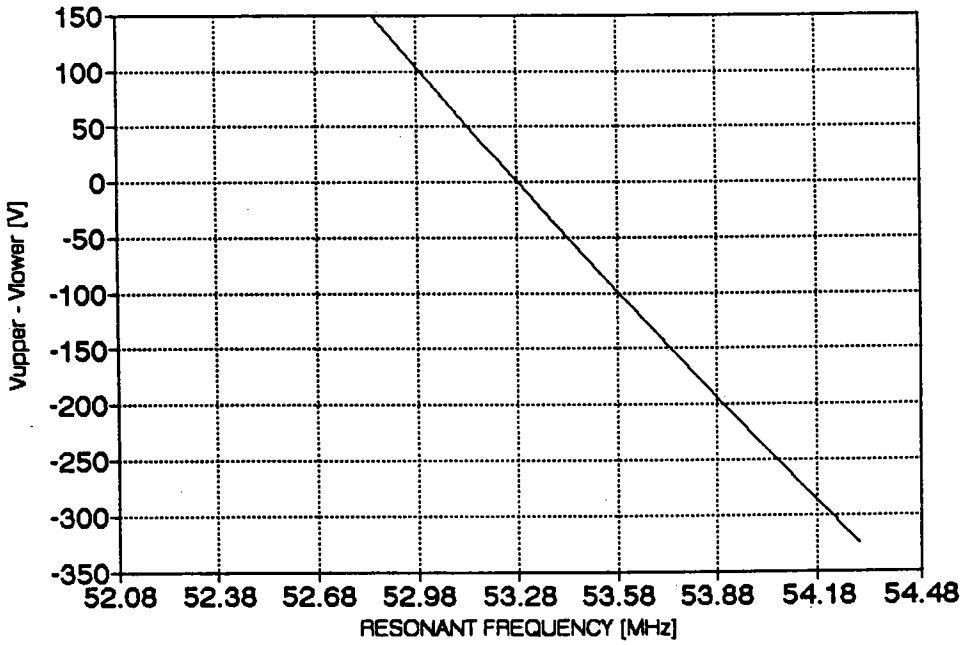

```
RESON file FLT4.DAT


; k500 3rd harmonic flat-topping study. 1/92
; inner conductor has (2) 1/4" water lines plus coupling
; line.
;
.UNIT centimeter
.COLUMNS 6
Vshort 3 0 0.0 0.0
TR11 3 4 0  Z0=125.3  WA=4.54  WC=32.99  L=6.0315
TR10 4 5 0  Z0=416.7  WA=5.9  WC=71.9  L=8.0
TR5A 5 6 0  Z0=59.4  WA=12.05  WC=24.6  L=9.6
TR6  6 7 0  Z0=57.3  WA=11.8  WC=26.0  L=13.85
TR7  7 8 0  Z0=59.2  WA=10.3  WC=22.9  L=9.0
TR8  8 9 0  Z0=67.4  WA=14.45  WC=22.75  L=17.5
TR9  9 10 0  Z0=88.5  WA=5.75  WC=10.95  L=23.25
TR5B 5 11 0  Z0=59.4  WA=12.05  WC=24.6  L=6.1
TR4  11 12 0  Z0=69.4  WA=9.75  WC=24.0  L=11.1
TR3  12 13 0  Z0=71.2  WA=8.35  WC=19.45  L=9.0
TR2  13 14 0  Z0=80.7  WA=6.69  WC=14.27  L=8.15
TR1  14 15 0  Z0=74.1  WA=5.0  WC=9.3  L=7.45
; terminating capacitances
CH   15 0 0.1pF
CT   10 0 0.1pF
I1  15 0 53.0mA 0.0
;.AC LIN 21 53.275MHz 53.285MHz
;.AC LIN 51 53.2MHz 53.3MHz
;.PRINT AC Vm(5) Vp(5) I(Vshort)
.REPORT AC 53.28MHz
.OUTPUT 0 "" TR $ P VD(1) ID(1)
```

```
RESON file FLT5.DAT


; k500 3rd harmonic flat-topping study. 1/92
; Inner conductor of (2) 1/4" water lines plus coupling
; line.
; Two coupled dees.
;
.UNIT centimeter
.PRECISION 8 6
.COLUMNS 6
Vshort 1 0 0.0 0.0
; tl11 in two pieces for direct coupling
;TR11A 1 99 0  Z0=125.3  WA=4.54  WC=32.99  L=0.6436
;TR11B 99 2 0  Z0=125.3  WA=4.54  WC=32.99  L=4.0621
;
TR11 1 2 0  Z0=125.3  WA=4.54  WC=32.99  L=4.7057
TR10 2 3 0  Z0=416.7  WA=5.9  WC=71.9  L=8.4
TR5A 3 4 0  Z0=59.4  WA=12.05  WC=24.6  L=9.6
TR6  4 5 0  Z0=57.3  WA=11.8  WC=26.0  L=13.85
TR7  5 6 0  Z0=59.2  WA=10.3  WC=22.9  L=9.0
TR8  6 7 0  Z0=67.4  WA=14.45  WC=22.75  L=17.5
TR9  7 8 0  Z0=88.5  WA=5.75  WC=10.95  L=23.25
TR5B 3 9 0  Z0=59.4  WA=12.05  WC=24.6  L=6.1
TR4  9 10 0  Z0=69.4  WA=9.75  WC=24.0  L=11.1
TR3  10 11 0  Z0=71.2  WA=8.35  WC=19.45  L=9.0
TR2  11 12 0  Z0=80.7  WA=6.69  WC=14.27  L=8.15
TR1  12 13 0  Z0=74.1  WA=5.0  WC=9.3  L=7.45
; drive current
I1  3 0 110.669mA 0.0
;
; lower dee
VshrtL 21 0 0.0 0.0
TR11L  21 22 0  Z0=125.3  WA=4.54  WC=32.99  L=4.7057
TR10L  22 23 0  Z0=416.7  WA=5.9  WC=71.9  L=8.4
TR5AL  23 24 0  Z0=59.4  WA=12.05  WC=24.6  L=9.6
TR6L   24 25 0  Z0=57.3  WA=11.8  WC=26.0  L=13.85
TR7L   25 26 0  Z0=59.2  WA=10.3  WC=22.9  L=9.0
TR8L   26 27 0  Z0=67.4  WA=14.45  WC=22.75  L=17.5
TR9L   27 28 0  Z0=88.5  WA=5.75  WC=10.95  L=23.25
TR5BL  23 29 0  Z0=59.4  WA=12.05  WC=24.6  L=6.1
TR4L   29 30 0  Z0=69.4  WA=9.75  WC=24.0  L=11.1
TR3L   30 31 0  Z0=71.2  WA=8.35  WC=19.45  L=9.0
TR2L   31 32 0  Z0=80.7  WA=6.69  WC=14.27  L=8.15
TR1L   32 33 0  Z0=74.1  WA=5.0  WC=9.3  L=7.45
;
; coupling capacitances
C1 7 27  5pF
C2 6 26  9pF
C3 5 25  9pF
C4 4 24 10pF
C5 3 23  8pF
C6 9 29  9pF
C7 10 30 9pF
C8 11 31 7pF
C9 12 32 4pF
;     tip capacitances
CH  13 0 0.1pF
CT  8 0 0.1pF
CHL 33 0 0.1pF
CHT 28 0 0.1pF
;     input coupler
;TCin 99 40 0 Ri=0.0975 Ro=0.2025 E=1.3 L=281.5
;Vdrv 41  0  566.0 0.0
;Rdrv 40 41 50.00
;Idrv 99 0 14.453 0.0
;
; output
;.AC LIN 21 29.208MHz 29.212MHz
;.PRINT AC V(3) Vp(3) V(23) Vp(23)
;.AC LIN 21 52.275MHz 52.285MHz
;.PRINT AC V(3) Vp(3) V(23) Vp(23)
.REPORT AC 53.28MHz
.OUTPUT 1 "even mode" all $ P VDm(1) VDp(1) IDm(1) IDp(1)
;.COUPLE 1 "50 OHM COUPLING POINT" Tname=TR11 Z0=50
;.REPORT AC 29.2092MHz
;.OUTPUT 1 "odd mode" ALL $ P VDm(1) VDp(1)
```

Appendix C. Coupling Calculations.

1. Determining Loop Area.

Figure C.1 is used for the analysis of the EMF generated in an arbitrary square loop located in a shorted section of air-filled coaxial transmission line. The surface vector of the loop is assumed to be ø-oriented, so the figure depicts a radial slice of the line. The center of the transmission line runs along the z-axis, with the short occurring at z=0. A current I(z) is assumed to run along the surface of each conductor, and the loop is delimited by the variables a,b,c,d. The H-field in a coaxial cylinder can easily be determined from Ampere's Law which gives

$$H_\phi(r,z) = \frac{I_0(z)}{2\pi r} e^{j\omega t}$$

For the arrangement in the figure we have only a ø-directed component of the H-field. The relationship between the magnetic flux and the emf generated around the loop is given by Faraday's Law as

$$\varepsilon = \oint \bar{E}\cdot d\bar{l} = -\frac{\partial}{\partial t}\int \bar{B}\cdot d\bar{S}$$

Taking the time-dependent variables outside the integral, and using the relation

$$d\bar{S} = dr\,dz\,\hat{\phi}$$

the expression for emf becomes

$$\varepsilon = -j\frac{\omega\mu}{2\pi} e^{j\omega t}\int \frac{I_0(z)}{r}\,dr\,dz$$

This expression can then be integrated over r.

$$\varepsilon = -j\frac{\omega\mu}{2\pi} e^{j\omega t}\ln\left(\frac{d}{c}\right)\int_a^b I_0(z)\,dz$$

If we then assume the section of line is of constant characteristic impedance, the z-dependence of the current can be written

Figure C.1

Figure for determining flux through a square loop located inside a shorted coaxial transmission line.

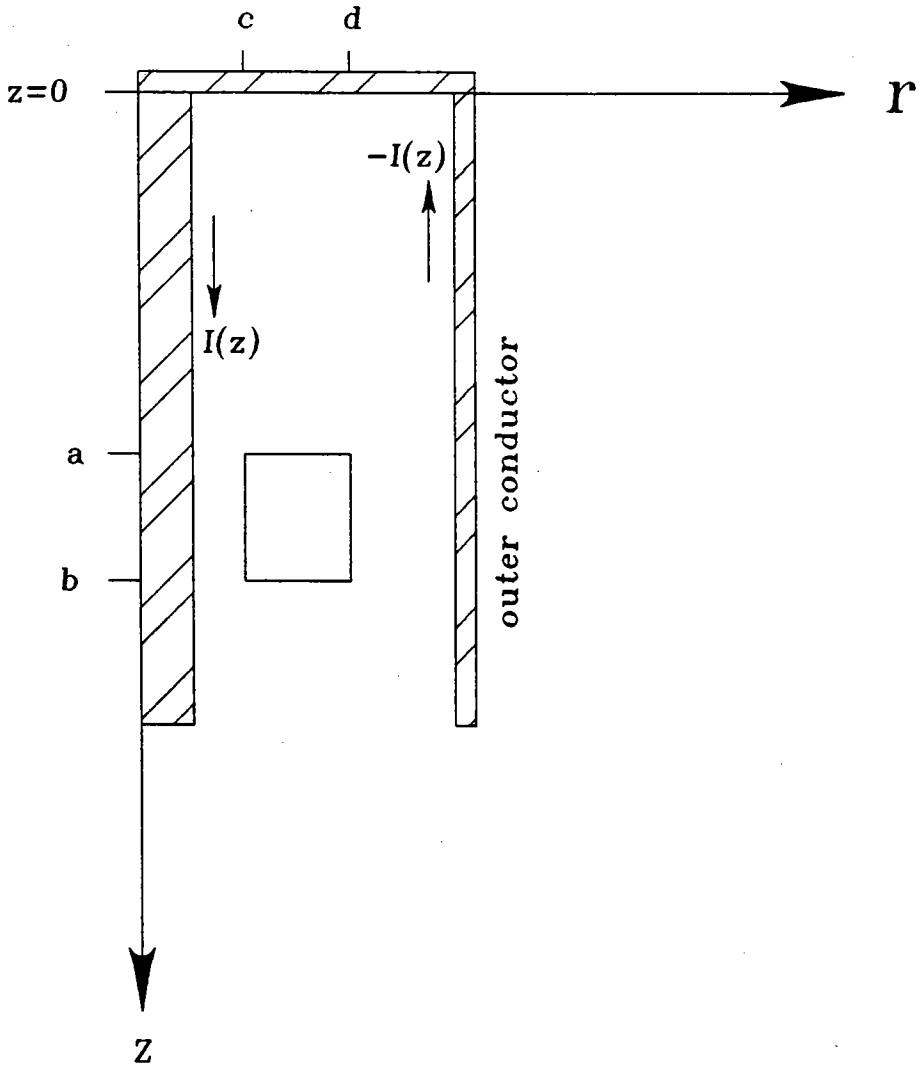

$$I_0(z) = I_s\cos(\beta z) \quad where \quad I_s = I_0(0)$$

Integrating this expression over z gives

$$\varepsilon = 60\, I_s \ln\left(\frac{d}{c}\right)[\sin(\beta b) - \sin(\beta a)]\, e^{j(\omega t - \frac{\pi}{2})}$$

where the following substitution has been made

$$\frac{\mu c}{2\pi} = 60$$

From this we then have an expression for the emf around the loop as a function of the flux enclosed by the loop, where this flux is determined by knowing the current distribution and loop position. Equating the peak loop voltage to the emf we get

$$V_{pk} = |\Re(\varepsilon)| = \frac{I_s \mu c}{2\pi} \ln\left(\frac{d}{c}\right)[\sin(\beta b) - \sin(\beta a)]$$

To match the cavity to a 50 Ohm line the impedance of the loop must equal 50 Ohms at resonance. In other words, the peak voltage across the loop is determined by the relation

$$\frac{V_{pk}^2}{2Z_0} = \langle P_D \rangle$$

where $\langle P_D \rangle$ = *time avg. power dissipated in the cavity*

and Z_0 *is the characteristic impedance of the line.*

If we equate the two relations above we find the relationship which defines the loop size in terms of the known cavity parameters.

$$\frac{\sqrt{2\langle P_D \rangle Z_0}}{60 I_s} = \ln\left(\frac{d}{c}\right)[\sin(\beta b) - \sin(\beta a)]$$

Using this relation we can determine a probable location for the loop. A possible shape for the loop would be a square formed from the center conductor up to the shorting plane, since this could be accurately machined as an integral part of the short. Figure C.3 shows the location of this loop with dimensions in centimeters of a=0, b=0.945, c=0.3175, and d=1.3175. The loop conductor width is about 0.3 cm and has 6-7 A rms passing through it.

2. Variations Affecting Loop Dimensions.

The loop designed above will be matched to the line for only one frequency at a given power dissipation. The sensitivity of the loop dimensions to a variation of parameters such as power dissipated and the resonant frequency can be determined through RESON simulations and the expression developed above. If we assume a possible variation in power of 20% up or down, this will account for the largest shift in the loop dimensions.

A change in resonant frequency changes both the distribution of the fields and the losses. If we assume that the change in f0 is less than 5%, the effect of this shift can be associated with a change in the current through the short. Variations in current of this magnitude cause less of a fluctuation in the loop dimensions, than the power related changes.

Looking at the numbers associated with these potential fluctuations, a first order design rule would be to allow a 50% change in the loop area from its nominal dimensions shown in figure C.3. A method for varying the loop size or its angle with respect to the magnetic flux will have to be implemented so tuning can be accomplished from outside the dees.

Figure C.2 Crossection of K500 upper dee at the dee shell - stem interface.

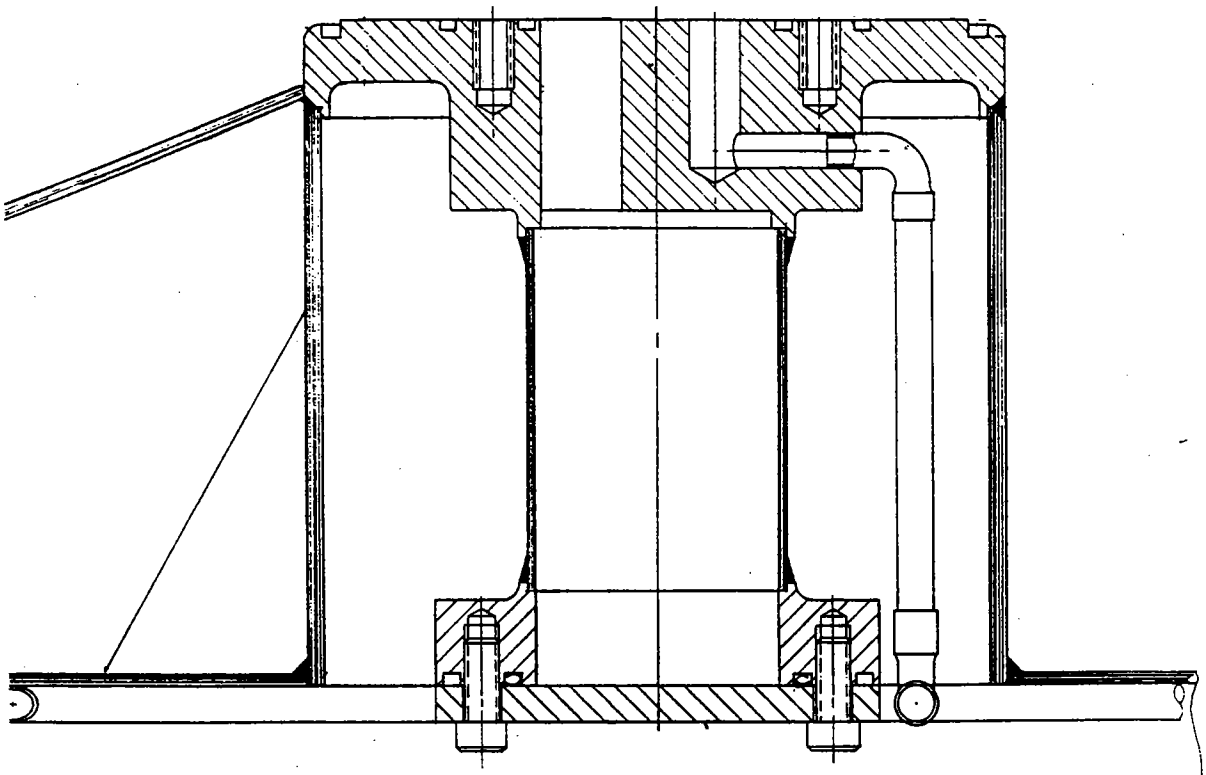

FIGURE C.3 LOOP COUPLER AND SUB-DEE SHORT

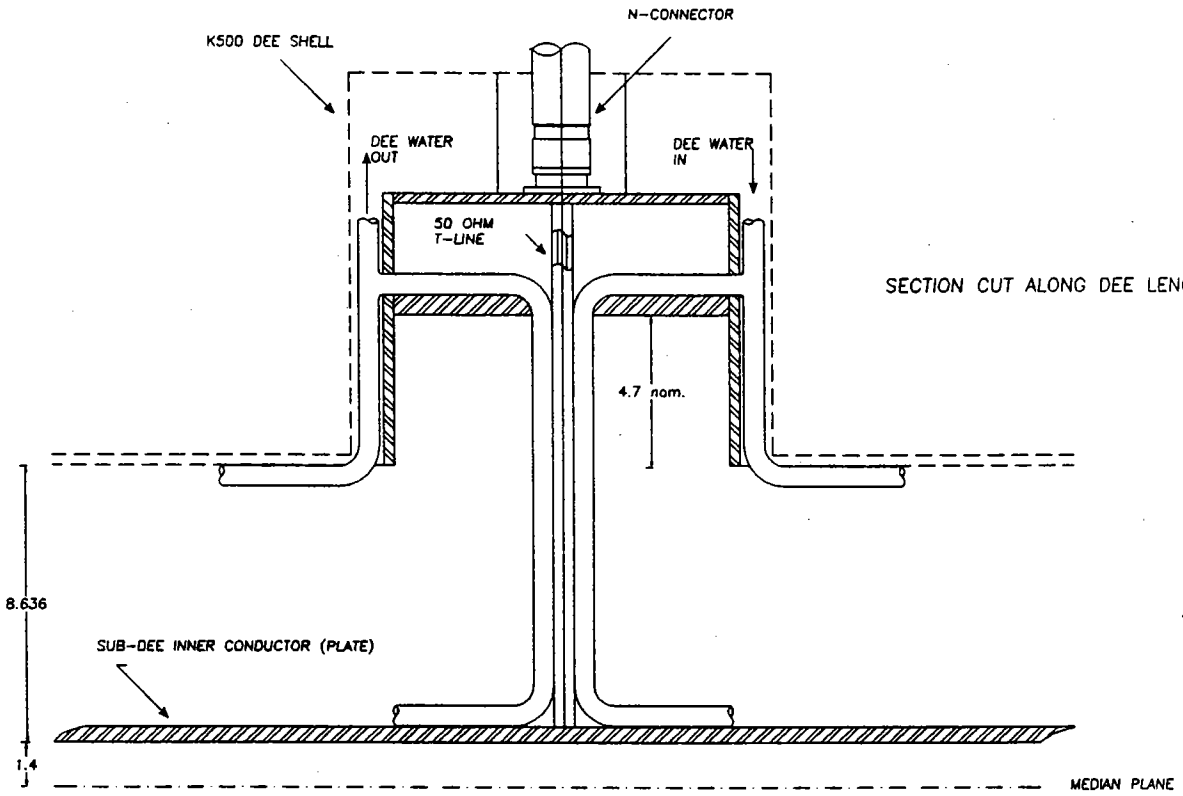

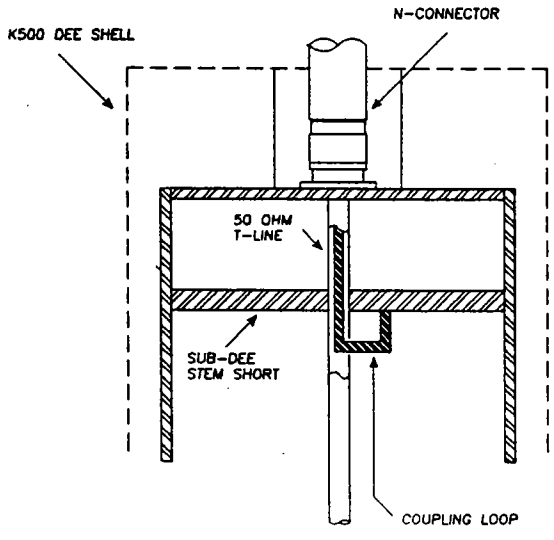

SECTION TRANSVERSE TO ABOVE FIGURE

Appendix D. POISSON/RFA Crossections.

PROB. NAME = K500 3RD HARM. - SECTION E1 CYCLE = 0
XMIN: 0.000, XMAX: 27.400
YMIN: 0.000, YMAX: 10.000

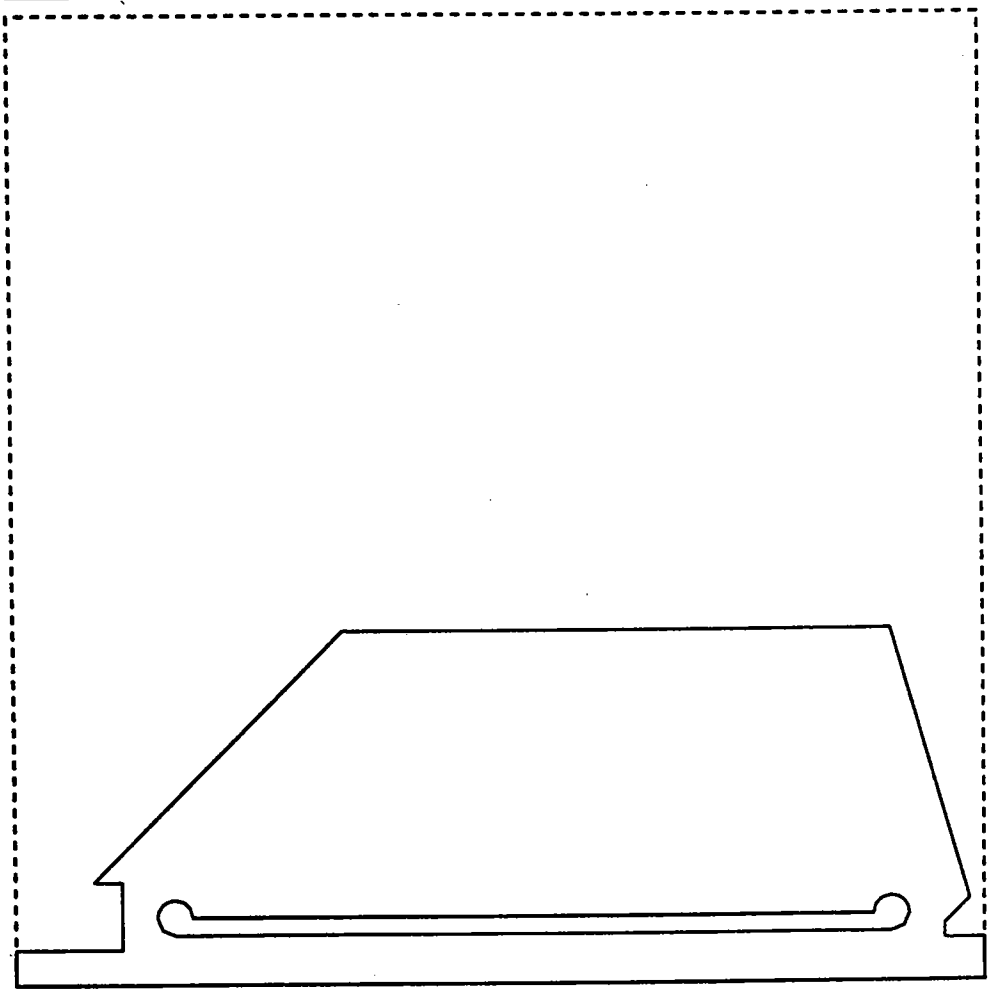

PROB. NAME = K500 3RD HARM. - SECTION F1 CYCLE = 0
XMIN: 0.000, XMAX: 15.000
YMIN: 0.000, YMAX: 10.000

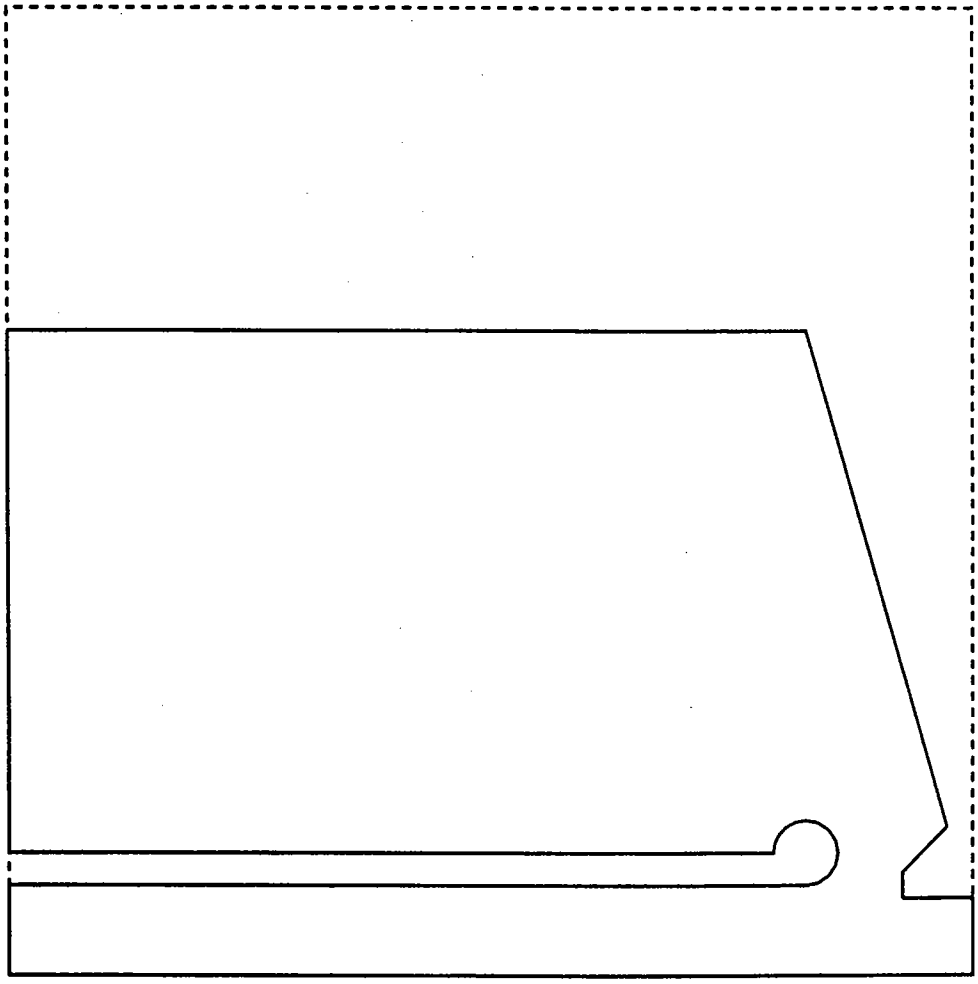

PROB. NAME = K500 3RD HARM. - SECTION G1 CYCLE = 0
XMIN: 0.000, XMAX: 12.900
YMIN: 0.000, YMAX: 10.000

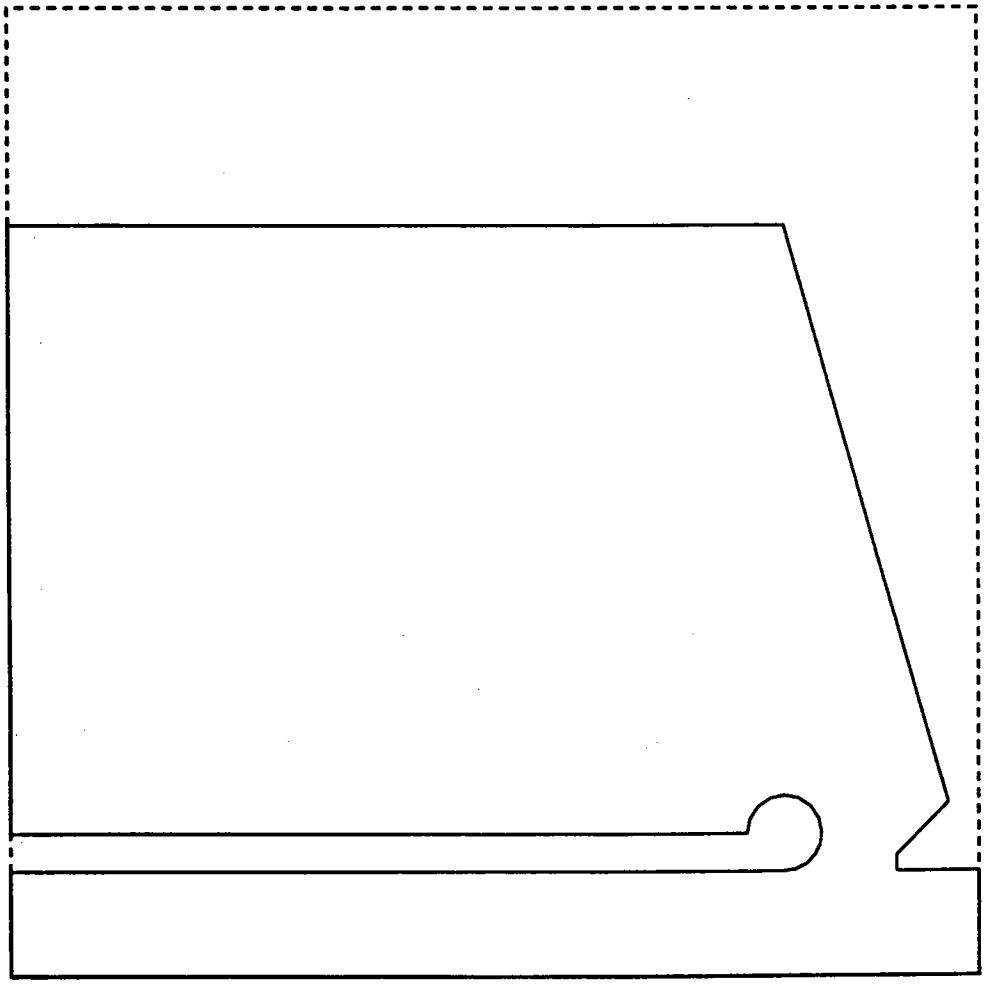

PROB. NAME = K500 3RD HARM. - SECTION H1 CYCLE = 0
XMIN: 0.000, XMAX: 11.000
YMIN: 0.000, YMAX: 10.000

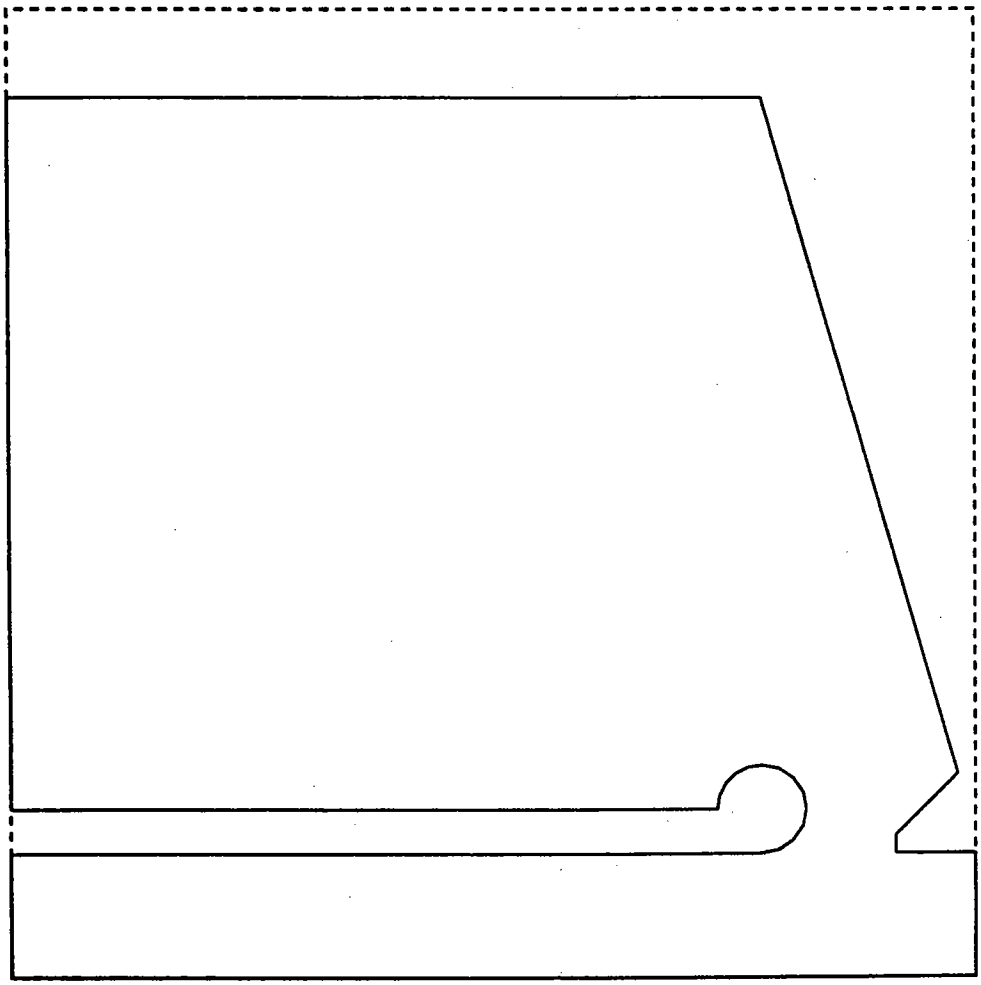

PROB. NAME = K500 3RD HARM. - SECTION J1 CYCLE = 0
XMIN: 0.000, XMAX: 9.600
YMIN: 0.000, YMAX: 10.000

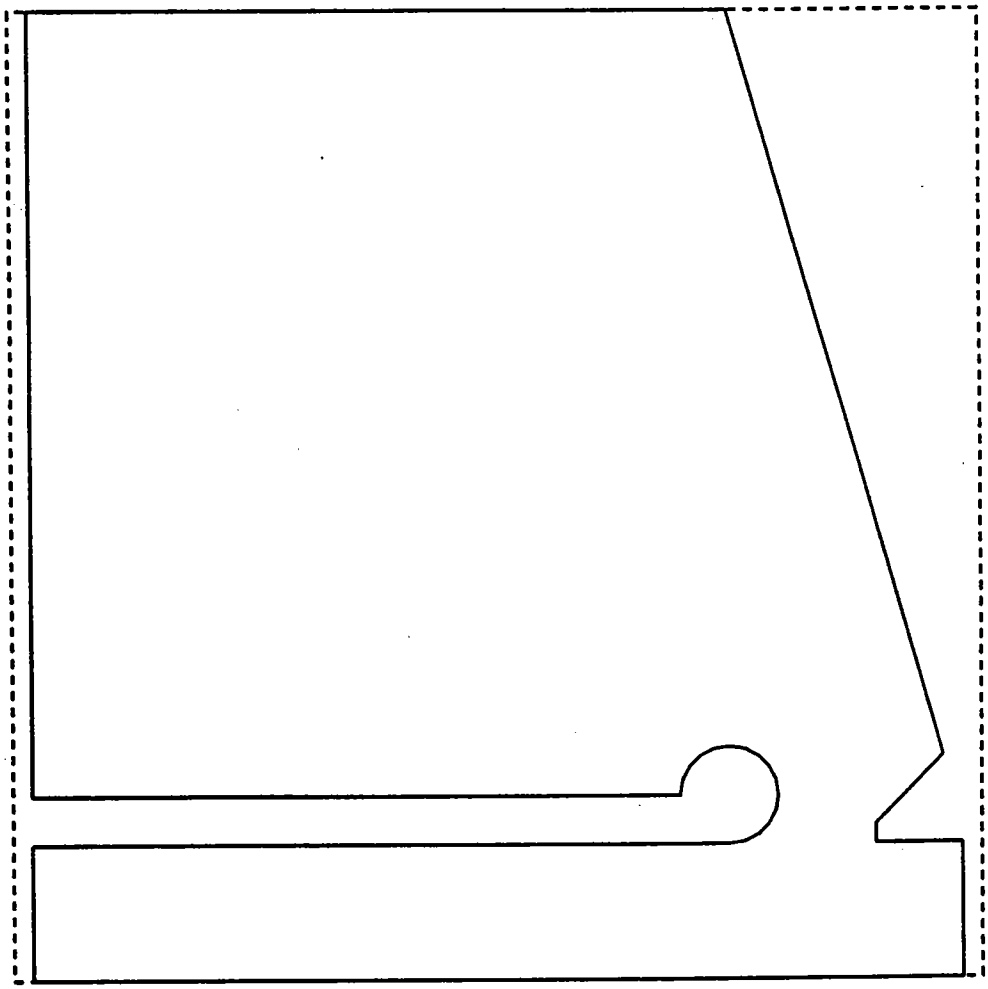

PROB. NAME = K500 3RD HARM. - SECTION K1 CYCLE = 0
XMIN: 0.000, XMAX: 7.100
YMIN: 0.000, YMAX: 10.000

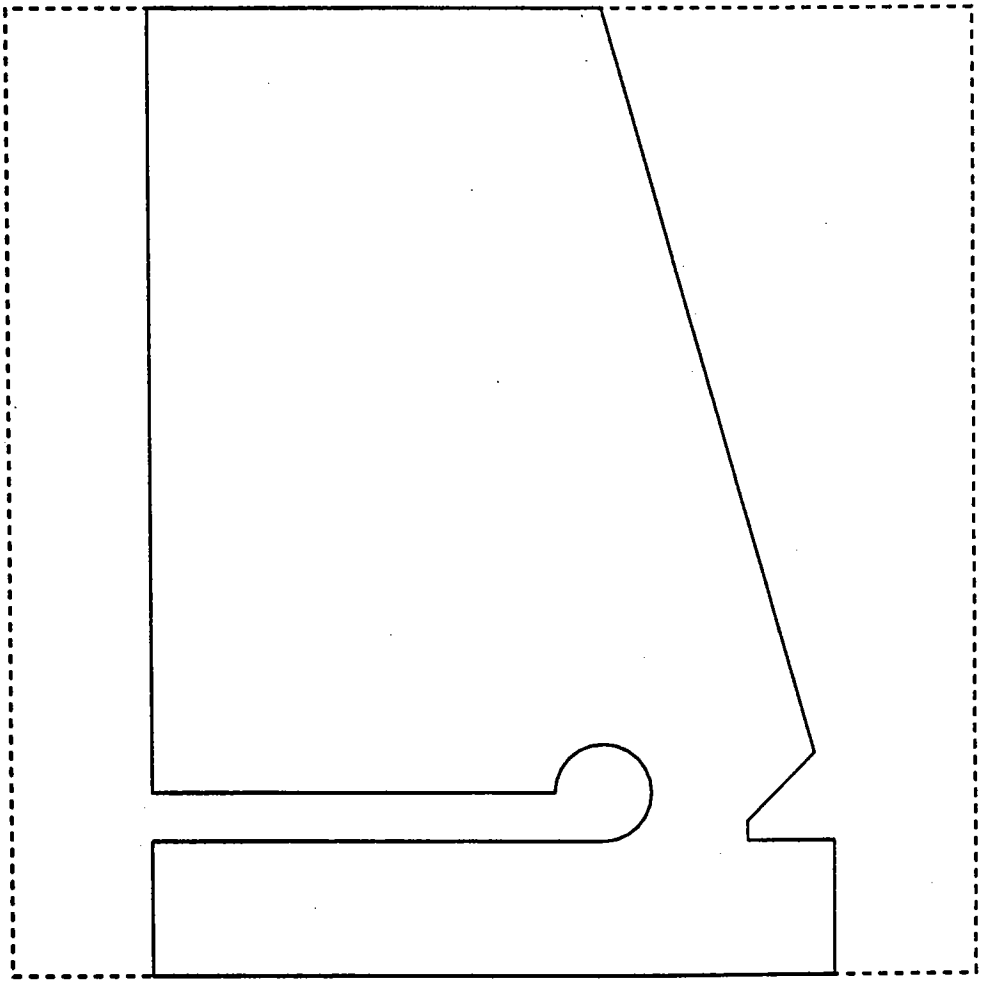

PROB. NAME = K500 3RD HARM. - SECTION L1 CYCLE = 0
XMIN: 0.000, XMAX: 8.500
YMIN: 0.000, YMAX: 10.000

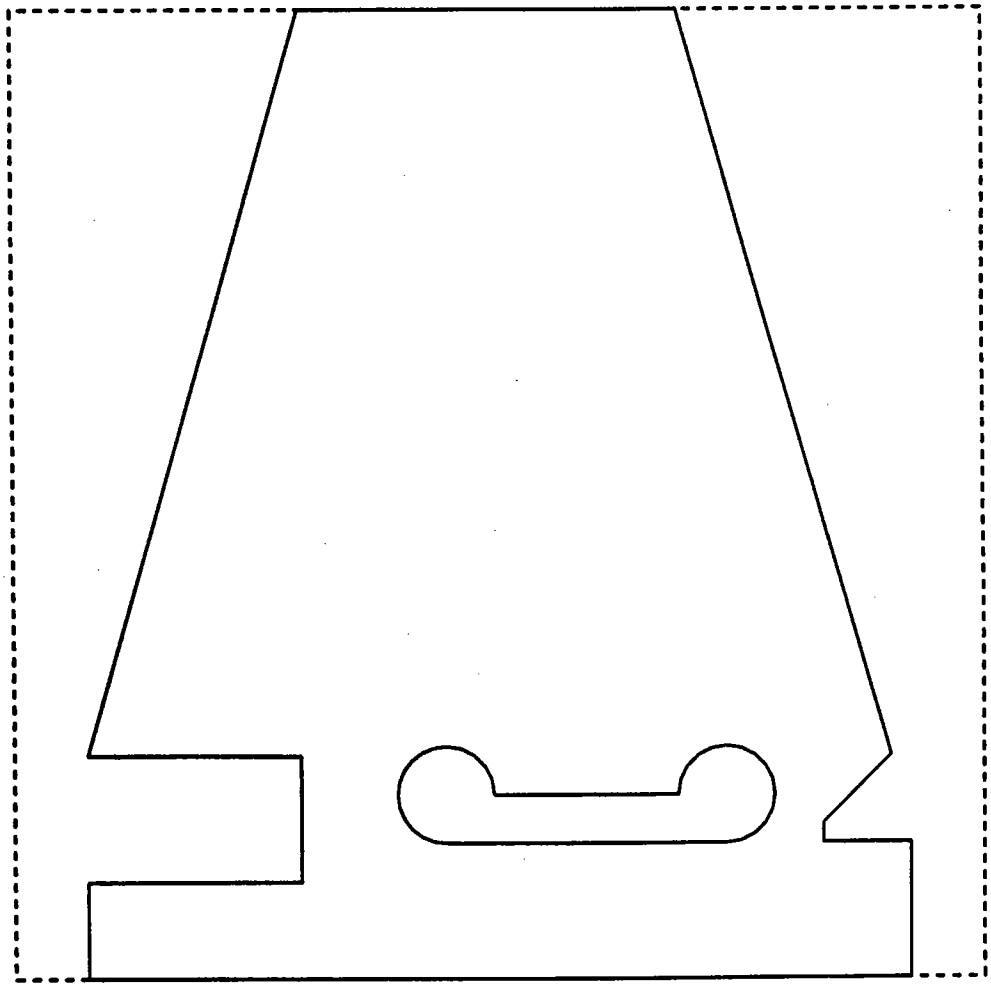

PROB. NAME = K500 3RD HARM. TEST - SECTION M CYCLE = 0
XMIN: 0.000, XMAX: 20.900
YMIN: 0.000, YMAX: 10.000

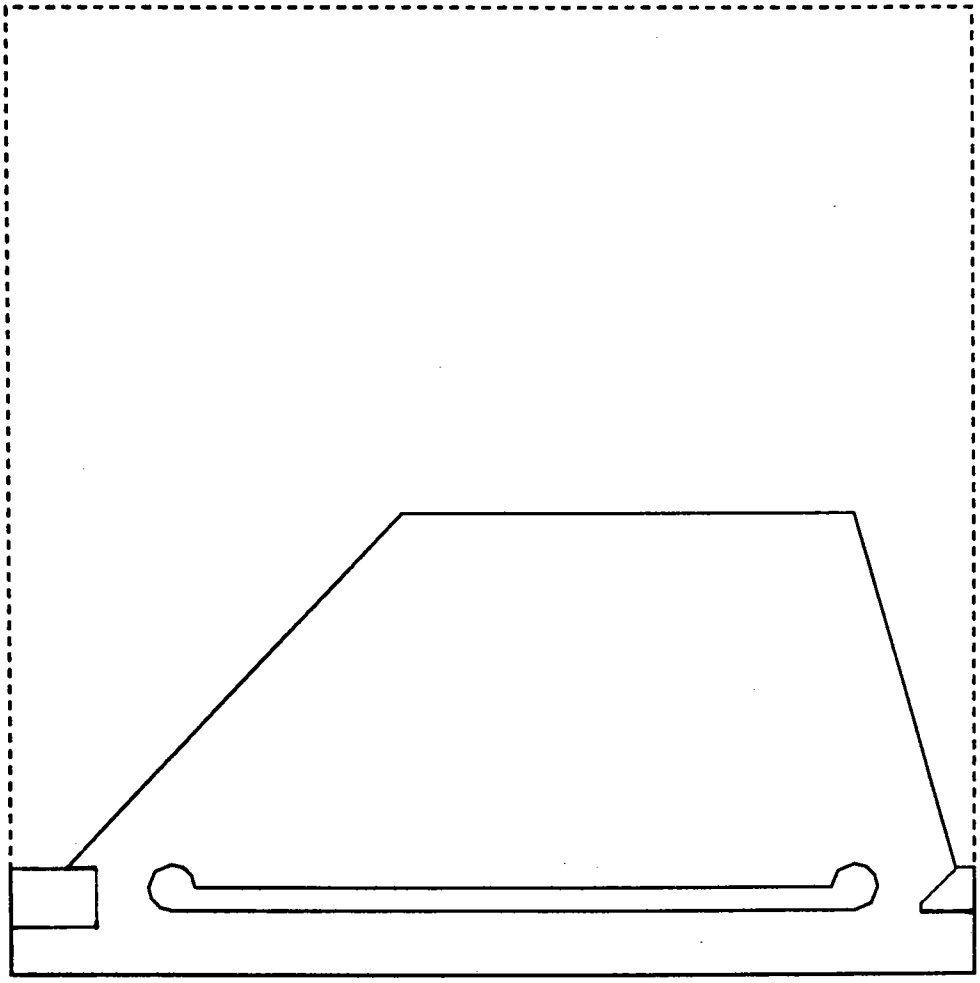

PROB. NAME = K500 3RD HARM. - SECTION P1 CYCLE = 0
XMIN: 0.000, XMAX: 9.200
YMIN: 0.000, YMAX: 7.400

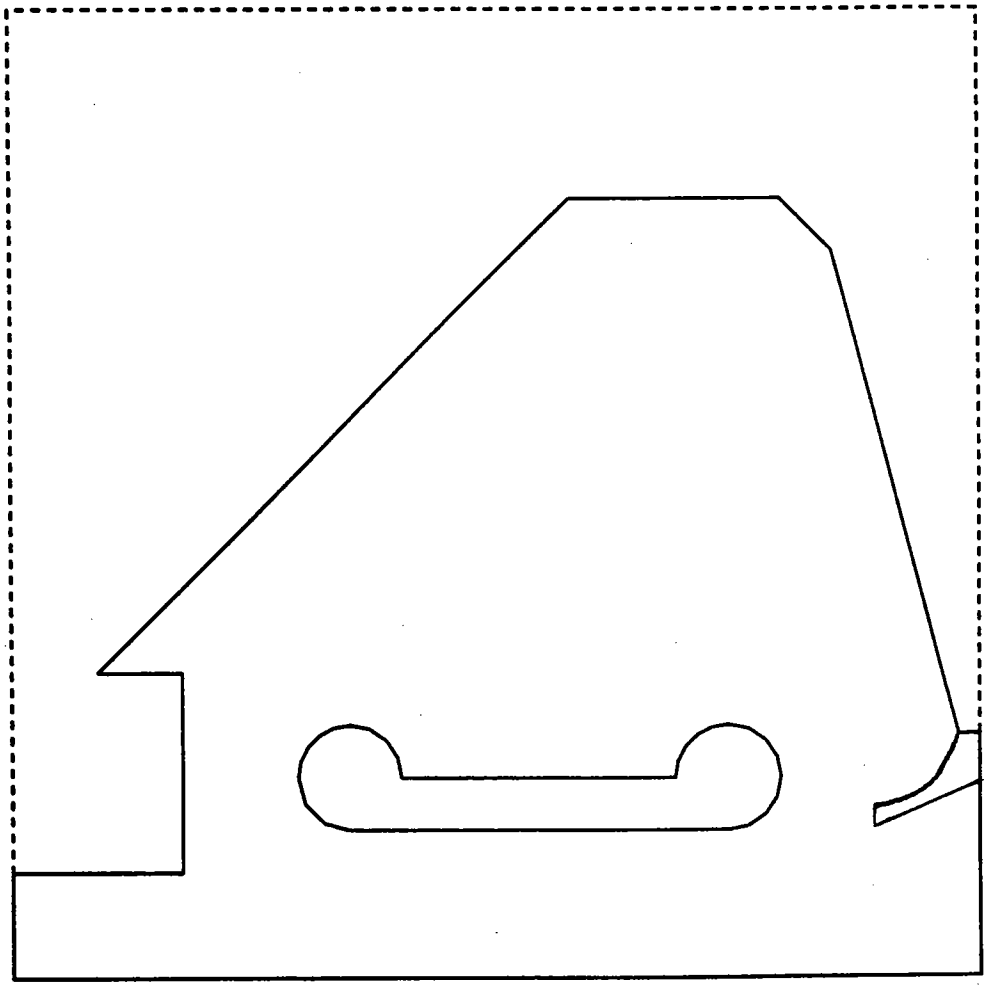

PROB. NAME = K500 3RD HARM. - SECTION X1 CYCLE = 0
XMIN: 0.000, XMAX: 46.000
YMIN: 0.000, YMAX: 46.000

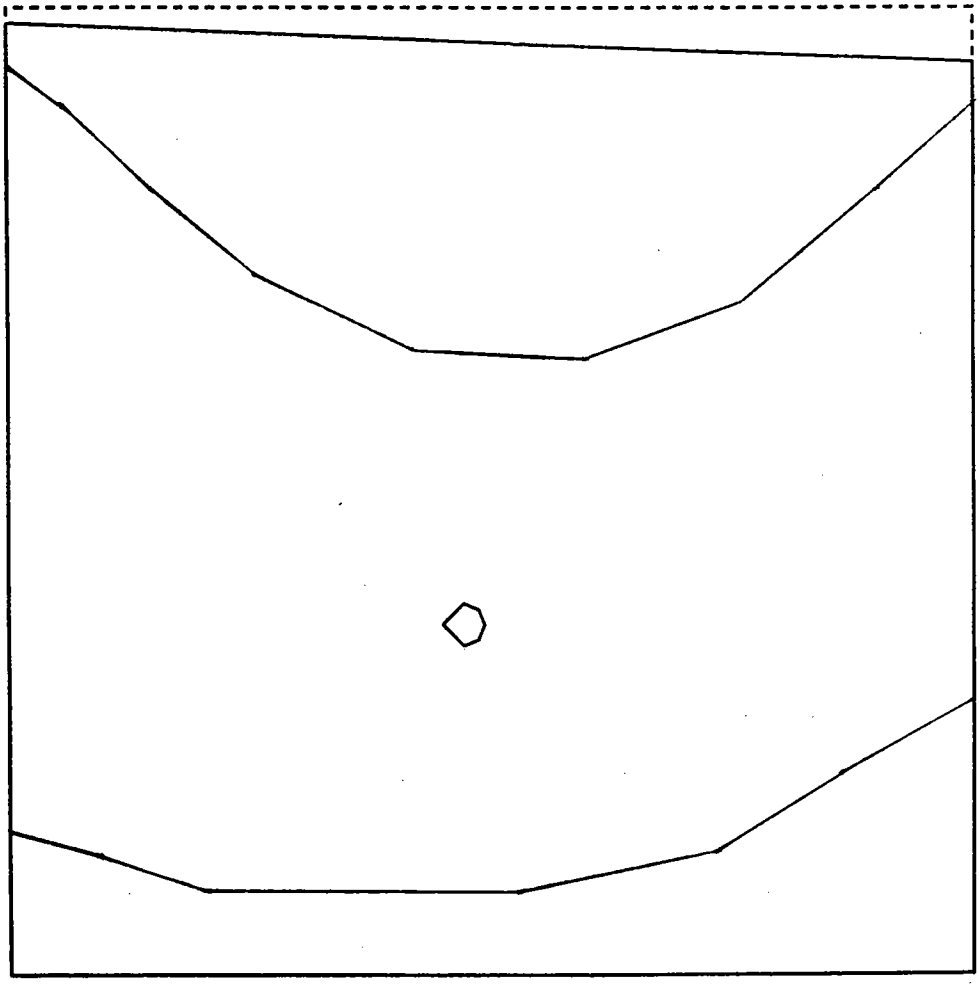

PROB. NAME = K500 3RD HARM. - SECTION Y4 CYCLE = 0
XMIN: 0.000, XMAX: 5.250
YMIN: 0.000, YMAX: 5.250

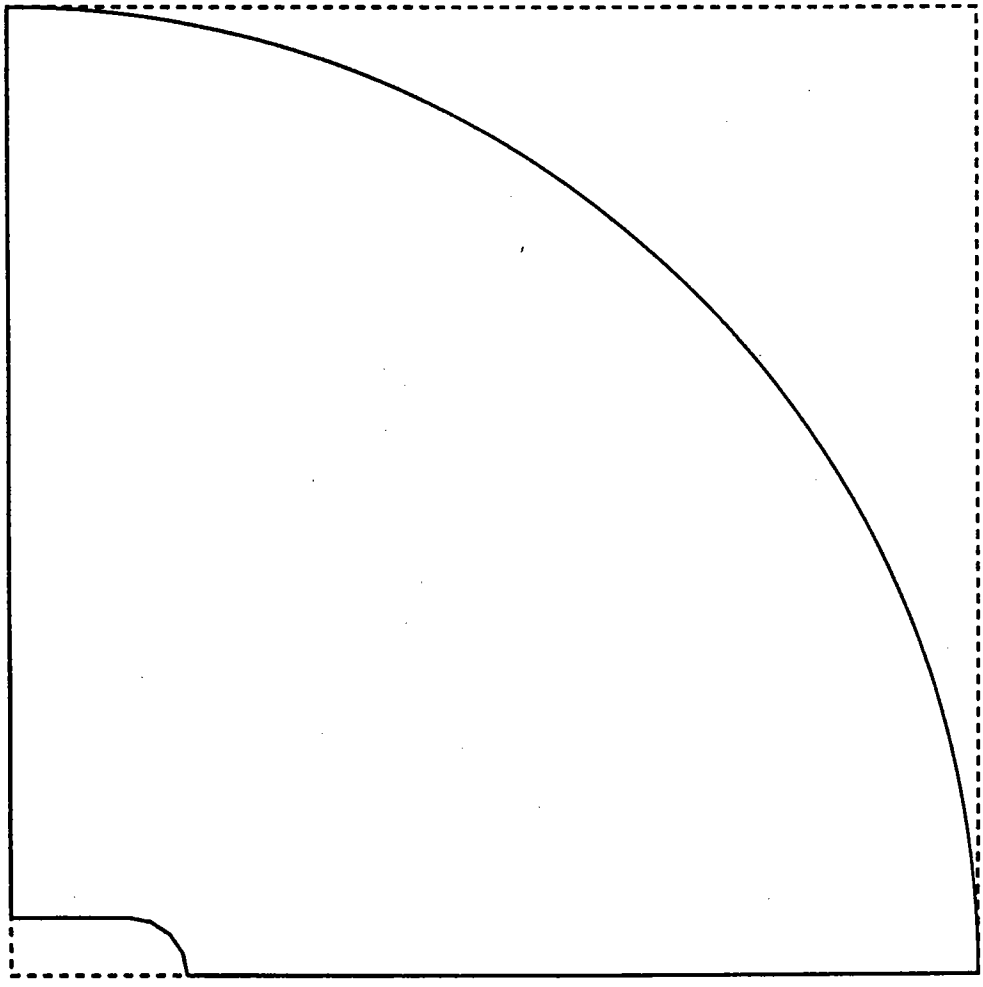

Appendix E. POISSON/RFA Input Files.

```
 K500 3RD HARM. - SECTION Y4
$REG NREG=3, DX=0.1, DY=0.1,
XMAX=5.25, YMAX=5.25,
NPOINT=6, MAT=1, $END
$PO X=0.0, Y=5.25, $END
$PO R=5.25, THETA=0.0, NT=2, $END
$PO R=0.3175, THETA=0.0, X0=0.635, Y0=0.0, NT=1, $END
$PO R=0.3175, THETA=90.0, X0=0.635, Y0=0.0, NT=2, $END
$PO X=0.0, Y=0.3175, $END
$PO X=0.0, Y=5.25, $END
$REG NPOINT=2, MAT=0, CUR=0.0, IBOUND=-1, $END
$PO X=0.0, Y=5.25, $END
$PO R=5.25, THETA=0.0, NT=2, $END
$REG NPOINT=3, MAT=0, CUR=1.0, IBOUND=-1, $END
$PO R=0.3175, THETA=0.0, X0=0.635, Y0=0.0, NT=1, $END
$PO R=0.3175, THETA=90.0, X0=0.635, Y0=0.0, NT=2, $END
$PO X=0.0, Y=0.3175, $END
```

```
 K500 3RD HARM. - SECTION X1
$REG NREG=4, DX=1.0, DY=1.0,
XMAX=46.0, YMAX=46.0,
NPOINT=11.0, MAT=1, $END
$PO X=0.0, Y=0.0, $END
$PO X=0.0, Y=5.0, $END
$PO X=0.0, Y=7.85, $END
$PO X=0.0, Y=41.65, $END
$PO X=0.0, Y=45.25, $END
$PO X=46.0, Y=43.4, $END
$PO X=46.0, Y=40.4, $END
$PO X=46.0, Y=14.00, $END
$PO X=46.0, Y=10.95, $END
$PO X=46.0, Y=0.0, $END
$PO X=0.0, Y=0.0, $END
$REG NPOINT=8, MAT=0, CUR=0.0, IBOUND=-1, $END
$PO X=0.0, Y=7.0, $END
$PO X=4.3, Y=6.0, $END
$PO X=9.5, Y=4.0, $END
$PO X=15.9, Y=4.0, $END
$PO X=24.4, Y=4.0, $END
$PO X=34.0, Y=6.0, $END
$PO X=40.4, Y=10.0, $END
$PO X=46.0, Y=13.0, $END
$REG NPOINT=5, MAT=0, CUR=1.0, IBOUND=-1, $END
$PO R=1.0, THETA=0.0, X0=21.7, Y0=16.7, NT=2, $END
$PO R=1.0, THETA=90.0, X0=21.7, Y0=16.7, NT=2, $END
$PO R=1.0, THETA=180.0, X0=21.7, Y0=16.7, NT=2, $END
$PO R=1.0, THETA=270.0, X0=21.7, Y0=16.7, NT=2, $END
$PO R=1.0, THETA=0.0, X0=21.7, Y0=16.7, NT=2, $END
$REG NPOINT=9, MAT=0, CUR=0.0, IBOUND=-1, $END
$PO X=0.0, Y=43.0, $END
$PO X=2.5, Y=41.0, $END
$PO X=7.0, Y=37.0, $END
$PO X=12.0, Y=33.0, $END
$PO X=19.3, Y=30.0, $END
$PO X=27.5, Y=29.0, $END
$PO X=35.0, Y=32.0, $END
$PO X=41.3, Y=37.0, $END
$PO X=46.0, Y=41.0, $END
```

```
 K500 3RD HARM. - SECTION P1
$REG NREG=3,DX=0.2,DY=0.2,
XMAX=9.2, YMAX=7.4,
NPOINT=13, MAT=1, $END
$PO X=5.0   ,Y=0.0   , $END
$PO X=0.0   ,Y=0.0   , $END
$PO X=0.0   ,Y=1.0   , $END
$PO X=1.6   ,Y=1.0   , $END
$PO X=1.6   ,Y=2.9   , $END
$PO X=0.8   ,Y=2.9   , $END
$PO X=5.3   ,Y=7.4   , $END
$PO X=7.3   ,Y=7.4   , $END
$PO X=7.8   ,Y=6.9   , $END
$PO X=9.0   ,Y=2.3   , $END
$PO X=9.2   ,Y=2.3   , $END
$PO X=9.2   ,Y=0.0   , $END
$PO X=5.0   ,Y=0.0   , $END
$REG NPOINT=11, MAT=0, CUR=0.0, IBOUND=-1, $END
$PO X=0.0   ,Y=1.0   , $END
$PO X=1.6   ,Y=1.0   , $END
$PO X=1.6   ,Y=2.9   , $END
$PO X=0.8   ,Y=2.9   , $END
$PO X=5.3   ,Y=7.4   , $END
$PO X=7.3   ,Y=7.4   , $END
$PO X=7.8   ,Y=6.9   , $END
$PO X=9.0   ,Y=2.3   , $END
$PO R=0.7, THETA=-90.0, X0=8.3, Y0=2.3, NT=2, $END
$PO X=8.3   ,Y=1.4   ,$END
$PO X=9.2   ,Y=1.8   ,$END
$REG NPOINT=10, MAT=0, CUR=1.0, IBOUND=-1, $END
$PO X=5.0, Y=1.4, $END
$PO X=6.8, Y=1.4, $END
$PO R=0.5, THETA=0.0, X0=6.8, Y0=1.9, NT=2, $END
$PO R=0.5, THETA=90.0, X0=6.8, Y0=1.9, NT=2, $END
$PO R=0.5, THETA=180.0, X0=6.8, Y0=1.9, NT=2, $END
$PO X=3.7, Y=1.9, $END
$PO R=0.5, THETA=90.0, X0=3.2, Y0=1.9, NT=2, $END
$PO R=0.5, THETA=180.0, X0=3.2, Y0=1.9, NT=2, $END
$PO R=0.5, THETA=270.0, X0=3.2, Y0=1.9, NT=2, $END
$PO X=5.0, Y=1.4, $END
```

```
 K500 3RD HARM. TEST - SECTION M
$REG NREG=3,DX=0.4,DY=0.2,
XMAX=20.9, YMAX=10.0,
NPOINT=9, MAT=1, $END
$PO X=0.0   ,Y=0.0   , $END
$PO X=20.9   ,Y=0.0   , $END
$PO X=20.9   ,Y=2.3   , $END
$PO X=20.5   ,Y=2.3   , $END
$PO X=18.3   ,Y=10.0   , $END
$PO X=8.5    ,Y=10.0   , $END
$PO X=1.2    ,Y=2.3   , $END
$PO X=0.0   ,Y=2.3   , $END
$PO X=0.0   ,Y=0.0   , $END
$REG NPOINT=10, MAT=0, CUR=0.0, IBOUND=-1, $END
$PO X=20.9   ,Y=1.4   , $END
$PO X=19.8   ,Y=1.4   , $END
$PO X=19.8   ,Y=1.6   , $END
$PO X=20.5   ,Y=2.3   , $END
$PO X=18.3   ,Y=10.0   , $END
$PO X=8.5    ,Y=10.0   , $END
$PO X=1.2    ,Y=2.3   , $END
$PO X=2.0    ,Y=2.3   , $END
$PO X=2.0    ,Y=1.0   , $END
$PO X=0.0   ,Y=1.0   , $END
$REG NPOINT=10, MAT=0, CUR=1.0, IBOUND=-1, $END
$PO X=10.9, Y=1.4, $END
$PO X=18.3, Y=1.4, $END
$PO R=0.5, THETA=0.0, X0=18.3, Y0=1.9, NT=2, $END
$PO R=0.5, THETA=90.0, X0=18.3, Y0=1.9, NT=2, $END
$PO R=0.5, THETA=180.0, X0=18.3, Y0=1.9, NT=2, $END
$PO X=4.0, Y=1.9, $END
$PO R=0.5, THETA=90.0, X0=3.5, Y0=1.9, NT=2, $END
$PO R=0.5, THETA=180.0, X0=3.5, Y0=1.9, NT=2, $END
$PO R=0.5, THETA=270.0, X0=3.5, Y0=1.9, NT=2, $END
$PO X=10.9, Y=1.4, $END
```

```
 K500 3RD HARM. - SECTION L1
$REG NREG=3,DX=0.15,DY=0.15,
XMAX=8.5, YMAX=10.0,
YREG1=3.7,
NPOINT=17, MAT=1, $END
$PO X=0.0  ,Y=0.0  , $END
$PO X=8.5  ,Y=0.0  , $END
$PO X=8.5  ,Y=1.4  ,$END
$PO X=7.6  ,Y=1.4  ,$END
$PO X=7.6  ,Y=1.6  ,$END
$PO X=8.3  ,Y=2.3  , $END
$PO X=7.9  ,Y=3.7  , $END
$PO X=7.3  ,Y=5.8  , $END
$PO X=6.1  ,Y=10.0  , $END
$PO X=2.2  ,Y=10.0  , $END
$PO X=1.0  ,Y=5.8  , $END
$PO X=0.4  ,Y=3.7  , $END
$PO X=0.0  ,Y=2.3  , $END
$PO X=2.2  ,Y=2.3  , $END
$PO X=2.2  ,Y=1.0  , $END
$PO X=0.0  ,Y=1.0  , $END
$PO X=0.0  ,Y=0.0  , $END
$REG NPOINT=14, MAT=0, CUR=0.0, IBOUND=-1, $END
$PO X=8.5  ,Y=1.4  ,$END
$PO X=7.6  ,Y=1.4  ,$END
$PO X=7.6  ,Y=1.6  ,$END
$PO X=8.3  ,Y=2.3  , $END
$PO X=7.9  ,Y=3.7  , $END
$PO X=7.3  ,Y=5.8  , $END
$PO X=6.1  ,Y=10.0  , $END
$PO X=2.2  ,Y=10.0  , $END
$PO X=1.0  ,Y=5.8  , $END
$PO X=0.4  ,Y=3.7  , $END
$PO X=0.0  ,Y=2.3  , $END
$PO X=2.2  ,Y=2.3  , $END
$PO X=2.2  ,Y=1.0  , $END
$PO X=0.0  ,Y=1.0  , $END
$REG NPOINT=10, MAT=0, CUR=1.0, IBOUND=-1, $END
$PO X=4.9, Y=1.4, $END
$PO X=6.6, Y=1.4, $END
$PO R=0.5, THETA=0.0, X0=6.6, Y0=1.9, NT=2, $END
$PO R=0.5, THETA=90.0, X0=6.6, Y0=1.9, NT=2, $END
$PO R=0.5, THETA=180.0, X0=6.6, Y0=1.9, NT=2, $END
$PO X=4.2, Y=1.9, $END
$PO R=0.5, THETA=90.0, X0=3.7, Y0=1.9, NT=2, $END
$PO R=0.5, THETA=180.0, X0=3.7, Y0=1.9, NT=2, $END
$PO R=0.5, THETA=270.0, X0=3.7, Y0=1.9, NT=2, $END
$PO X=4.9, Y=1.4, $END
$REG NPOINT=2, MAT=0, CUR=0.0, IBOUND=-1, $END
$PO X=1.0, Y=5.8, $END
$PO X=7.3, Y=5.8, $END
$REG NPOINT=2, MAT=0, CUR=0.0, IBOUND=-1, $END
$PO X=0.4  ,Y=3.7  , $END
$PO X=7.9  ,Y=3.7  , $END
```

```
 K500 3RD HARM. - SECTION K1
$REG NREG=3,DX=0.2,DY=0.1,
XMAX=7.1, YMAX=10.0,
YREG1=4.4,
NPOINT=11, MAT=1, $END
$PO X=0.0  ,Y=0.0  , $END
$PO X=7.1 ,Y=0.0 , $END
$PO X=7.1 ,Y=1.4 , $END
$PO X=6.2 ,Y=1.4 , $END
$PO X=6.2 ,Y=1.6 , $END
$PO X=6.9 ,Y=2.3 , $END
$PO X=6.3 ,Y=4.4 , $END
$PO X=4.7  ,Y=10.0  , $END
$PO X=0.0  ,Y=10.0  , $END
$PO X=0.0  ,Y=4.4  , $END
$PO X=0.0  ,Y=0.0  , $END
$REG NPOINT=7, MAT=0, CUR=0.0, IBOUND=-1, $END
$PO X=7.1 ,Y=1.4 , $END
$PO X=6.2 ,Y=1.4 , $END
$PO X=6.2 ,Y=1.6 , $END
$PO X=6.9 ,Y=2.3 , $END
$PO X=6.3 ,Y=4.4 , $END
$PO X=4.7  ,Y=10.0  , $END
$PO X=0.0  ,Y=10.0  , $END
$REG NPOINT=7, MAT=0, CUR=1.0, IBOUND=-1, $END
$PO X=0.0, Y=1.4, $END
$PO X=4.7, Y=1.4, $END
$PO R=0.5, THETA=0.0, X0=4.7, Y0=1.9, NT=2, $END
$PO R=0.5, THETA=90.0, X0=4.7, Y0=1.9, NT=2, $END
$PO R=0.5, THETA=180.0, X0=4.7, Y0=1.9, NT=2, $END
$PO X=0.0, Y=1.9, $END
$PO X=0.0, Y=1.4, $END
```

```
 K500 3RD HARM. - SECTION J1
$REG NREG=3,DX=0.2,DY=0.12,
XMAX=9.6, YMAX=10.0,
YREG1=4.4,
NPOINT=11, MAT=1, $END
$PO X=0.0  ,Y=0.0  , $END
$PO X=9.6 ,Y=0.0 , $END
$PO X=9.6 ,Y=1.4 , $END
$PO X=8.7 ,Y=1.4 , $END
$PO X=8.7 ,Y=1.6 , $END
$PO X=9.4 ,Y=2.3 , $END
$PO X=8.8 ,Y=4.4  , $END
$PO X=7.2  ,Y=10.0  , $END
$PO X=0.0  ,Y=10.0  , $END
$PO X=0.0  ,Y=4.4  , $END
$PO X=0.0  ,Y=0.0  , $END
$REG NPOINT=7, MAT=0, CUR=0.0, IBOUND=-1, $END
$PO X=9.6 ,Y=1.4 , $END
$PO X=8.7 ,Y=1.4 , $END
$PO X=8.7 ,Y=1.6 , $END
$PO X=9.4 ,Y=2.3 , $END
$PO X=8.8 ,Y=4.4  , $END
$PO X=7.2  ,Y=10.0  , $END
$PO X=0.0  ,Y=10.0  , $END
$REG NPOINT=7, MAT=0, CUR=1.0, IBOUND=-1, $END
$PO X=0.0, Y=1.4, $END
$PO X=7.2, Y=1.4, $END
$PO R=0.5, THETA=0.0, X0=7.2, Y0=1.9, NT=2, $END
$PO R=0.5, THETA=90.0, X0=7.2, Y0=1.9, NT=2, $END
$PO R=0.5, THETA=180.0, X0=7.2, Y0=1.9, NT=2, $END
$PO X=0.0, Y=1.9, $END
$PO X=0.0, Y=1.4, $END
```

```
 K500 3RD HARM. - SECTION H1
$REG NREG=3,DX=0.2,DY=0.2,
XMAX=11.0, YMAX=10.0,
YREG1=4.4,
NPOINT=11, MAT=1, $END
$PO X=0.0  ,Y=0.0  , $END
$PO X=11.0 ,Y=0.0  , $END
$PO X=11.0 ,Y=1.4  , $END
$PO X=10.1 ,Y=1.4  , $END
$PO X=10.1 ,Y=1.6  , $END
$PO X=10.8 ,Y=2.3  , $END
$PO X=10.2 ,Y=4.4  , $END
$PO X=8.6  ,Y=10.0  , $END
$PO X=0.0  ,Y=10.0  , $END
$PO X=0.0  ,Y=4.4  , $END
$PO X=0.0  ,Y=0.0  , $END
$REG NPOINT=7, MAT=0, CUR=0.0, IBOUND=-1, $END
$PO X=11.0 ,Y=1.4  , $END
$PO X=10.1 ,Y=1.4  , $END
$PO X=10.1 ,Y=1.6  , $END
$PO X=10.8 ,Y=2.3  , $END
$PO X=10.2 ,Y=4.4  , $END
$PO X=8.6  ,Y=10.0  , $END
$PO X=0.0  ,Y=10.0  , $END
$REG NPOINT=7, MAT=0, CUR=1.0, IBOUND=-1, $END
$PO X=0.0, Y=1.4, $END
$PO X=8.6, Y=1.4, $END
$PO R=0.5, THETA=0.0, X0=8.6, Y0=1.9, NT=2, $END
$PO R=0.5, THETA=90.0, X0=8.6, Y0=1.9, NT=2, $END
$PO R=0.5, THETA=180.0, X0=8.6, Y0=1.9, NT=2, $END
$PO X=0.0, Y=1.9, $END
$PO X=0.0, Y=1.4, $END
```

```
 K500 3RD HARM. - SECTION G1
$REG NREG=3,DX=0.2,DY=0.15,
XMAX=12.9, YMAX=10.0,
YREG1=4.4,
NPOINT=11, MAT=1, $END
$PO X=0.0  ,Y=0.0   , $END
$PO X=12.9 ,Y=0.0 , $END
$PO X=12.9 ,Y=1.4 , $END
$PO X=11.8 ,Y=1.4 , $END
$PO X=11.8 ,Y=1.6 , $END
$PO X=12.5 ,Y=2.3 , $END
$PO X=11.9 ,Y=4.4 , $END
$PO X=10.3 ,Y=10.0   , $END
$PO X=0.0  ,Y=10.0   , $END
$PO X=0.0  ,Y=4.4   , $END
$PO X=0.0  ,Y=0.0   , $END
$REG NPOINT=7, MAT=0, CUR=0.0, IBOUND=-1, $END
$PO X=12.9 ,Y=1.4 , $END
$PO X=11.8 ,Y=1.4 , $END
$PO X=11.8 ,Y=1.6 , $END
$PO X=12.5 ,Y=2.3 , $END
$PO X=11.9 ,Y=4.4 , $END
$PO X=10.3 ,Y=10.0   , $END
$PO X=0.0  ,Y=10.0   , $END
$REG NPOINT=7, MAT=0, CUR=1.0, IBOUND=-1, $END
$PO X=0.0, Y=1.4, $END
$PO X=10.3, Y=1.4, $END
$PO R=0.5, THETA=0.0, X0=10.3, Y0=1.9, NT=2, $END
$PO R=0.5, THETA=90.0, X0=10.3, Y0=1.9, NT=2, $END
$PO R=0.5, THETA=180.0, X0=10.3, Y0=1.9, NT=2, $END
$PO X=0.0, Y=1.9, $END
$PO X=0.0, Y=1.4, $END
```

```
 K500 3RD HARM. - SECTION F1
$REG NREG=4,DX=0.2,DY=0.2,
XMAX=15.0, YMAX=10.0,
YREG1=4.4,
NPOINT=10, MAT=1, $END
$PO X=0.0  ,Y=0.0  , $END
$PO X=15.0 ,Y=0.0  , $END
$PO X=15.0 ,Y=1.2  , $END
$PO X=13.9 ,Y=1.2  , $END
$PO X=13.9 ,Y=1.6  , $END
$PO X=14.6 ,Y=2.3  , $END
$PO X=14.0 ,Y=4.4  , $END
$PO X=12.4 ,Y=10.0  , $END
$PO X=0.0  ,Y=10.0  , $END
$PO X=0.0  ,Y=0.0  , $END
$REG NPOINT=2, MAT=1, CUR=0.0, IBOUND=1, $END
$PO X=0.0, Y=4.4, $END
$PO X=14.0, Y=4.4, $END
$REG NPOINT=7, MAT=0, CUR=0.0, IBOUND=-1, $END
$PO X=15.0 ,Y=1.2  , $END
$PO X=13.9 ,Y=1.2  , $END
$PO X=13.9 ,Y=1.6  , $END
$PO X=14.6 ,Y=2.3  , $END
$PO X=14.0 ,Y=4.4  , $END
$PO X=12.4 ,Y=10.0  , $END
$PO X=0.0  ,Y=10.0  , $END
$REG NPOINT=7, MAT=0, CUR=1.0, IBOUND=-1, $END
$PO X=0.0, Y=1.4, $END
$PO X=12.4, Y=1.4, $END
$PO R=0.5, THETA=0.0, X0=12.4, Y0=1.9, NT=2, $END
$PO R=0.5, THETA=90.0, X0=12.4, Y0=1.9, NT=2, $END
$PO R=0.5, THETA=180.0, X0=12.4, Y0=1.9, NT=2, $END
$PO X=0.0, Y=1.9, $END
$PO X=0.0, Y=1.4, $END
```

```
 K500 3RD HARM. - SECTION E1
$REG NREG=4,DX=0.3,DY=0.2,
XMAX=27.4, YMAX=10.0,
YREG1=3.7,
NPOINT=15, MAT=1, $END
$PO X=0.0  ,Y=0.0  , $END
$PO X=27.4 ,Y=0.0  , $END
$PO X=27.4  ,Y=1.2  , $END
$PO X=26.3  ,Y=1.2  , $END
$PO X=26.3  ,Y=1.6  , $END
$PO X=27.0  ,Y=2.3  , $END
$PO X=26.6  ,Y=3.7  , $END
$PO X=24.8  ,Y=10.0  , $END
$PO X=9.3  ,Y=10.0  , $END
$PO X=3.0  ,Y=3.7  , $END
$PO X=2.2  ,Y=2.9  , $END
$PO X=3.0  ,Y=2.9  , $END
$PO X=3.0  ,Y=1.0  , $END
$PO X=0.0  ,Y=1.0  , $END
$PO X=0.0  ,Y=0.0  , $END
$REG NPOINT=12, MAT=0, CUR=0.0, IBOUND=-1, $END
$PO X=27.4  ,Y=1.2  , $END
$PO X=26.3  ,Y=1.2  , $END
$PO X=26.3  ,Y=1.6  , $END
$PO X=27.0  ,Y=2.3  , $END
$PO X=26.6  ,Y=3.7  , $END
$PO X=24.8  ,Y=10.0  , $END
$PO X=9.3  ,Y=10.0  , $END
$PO X=3.0  ,Y=3.7  , $END
$PO X=2.2  ,Y=2.9  , $END
$PO X=3.0  ,Y=2.9  , $END
$PO X=3.0  ,Y=1.0  , $END
$PO X=0.0  ,Y=1.0  , $END
$REG NPOINT=10, MAT=0, CUR=1.0, IBOUND=-1, $END
$PO X=10.1, Y=1.4, $END
$PO X=24.8, Y=1.4, $END
$PO R=0.5, THETA=0.0, X0=24.8, Y0=1.9, NT=2, $END
$PO R=0.5, THETA=90.0, X0=24.8, Y0=1.9, NT=2, $END
$PO R=0.5, THETA=180.0, X0=24.8, Y0=1.9, NT=2, $END
$PO X=5.0, Y=1.9, $END
$PO R=0.5, THETA=90.0, X0=4.5, Y0=1.9, NT=2, $END
$PO R=0.5, THETA=180.0, X0=4.5, Y0=1.9, NT=2, $END
$PO R=0.5, THETA=270.0, X0=4.5, Y0=1.9, NT=2, $END
$PO X=10.1, Y=1.4, $END
$REG NPOINT=2, MAT=1, CUR=0.0, IBOUND=1, $END
$PO X=3.0  ,Y=3.7  , $END
$PO X=26.6  ,Y=3.7  , $END
```